AD NUMBER

AD843332

LIMITATION CHANGES

TO:

Approved for public release; distribution is unlimited.

FROM:

Distribution authorized to U.S. Gov't. agencies and their contractors; Critical Technology; OCT 1968. Other requests shall be referred to Air Force Weapons Laboratory, Kirtland AFB, NM 87117. This document contains export-controlled technical data.

AUTHORITY

AFWL ltr, 30 Nov 1971

AFWL-TR-
68-96

EXPERIMENTAL RESEARCH ON COLLISIONS OF HEAVY PARTICLES AT ENERGIES UP TO 2 MeV

R. T. Brackman

W. L. Fite

University of Pittsburgh

Department of Physics

Pittsburgh, Pennsylvania

Contract No. F29601-67-C-0086

TECHNICAL REPORT NO. AFWL-TR-68-96

October 1968

AIR FORCE WEAPONS LABORATORY

Air Force Systems Command

Kirtland Air Force Base

New Mexico

DISCLAIMER NOTICE

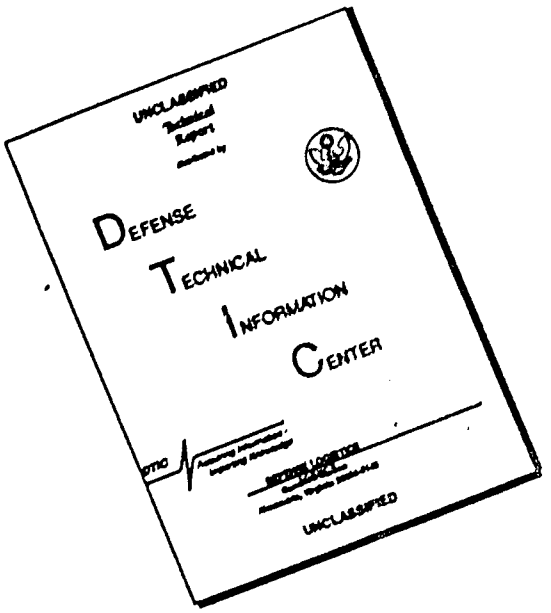

THIS DOCUMENT IS BEST QUALITY AVAILABLE. THE COPY FURNISHED TO DTIC CONTAINED A SIGNIFICANT NUMBER OF PAGES WHICH DO NOT REPRODUCE LEGIBLY.

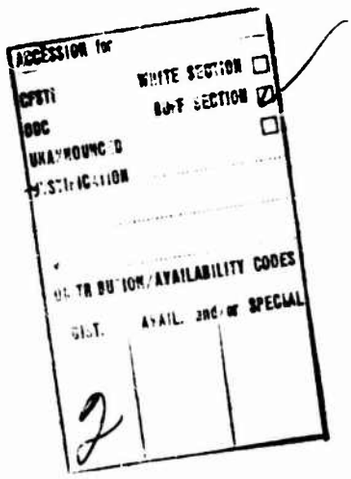

AIR FORCE WEAPONS LABORATORY
Air Force Systems Command
Kirtland Air Force Base
New Mexico

When U. S. Government drawings, specifications, or other data are used for any purpose other than a definitely related Government procurement operation, the Government thereby incurs no responsibility nor any obligation whatsoever, and the fact that the Government may have formulated, furnished, or in any way supplied the said drawings, specifications, or other data, is not to be regarded by implication or otherwise, as in any manner licensing the holder or any other person or corporation, or conveying any rights or permission to manufacture, use, or sell any patented invention that may in any way be related thereto.

This report is made available for study with the understanding that proprietary interests in and relating thereto will not be impaired. In case of apparent conflict or any other questions between the Government's rights and those of others, notify the Judge Advocate, Air Force Systems Command, Andrews Air Force Base, Washington, D. C. 20331.

DO NOT RETURN THIS COPY. RETAIN OR DESTROY.

AFWL-TR-68-96

EXPERIMENTAL RESEARCH ON COLLISIONS OF HEAVY PARTICLES AT ENERGIES UP TO 2 MeV

R. T. Brackman
W. L. Fite

University of Pittsburgh
Department of Physics
Pittsburgh, Pennsylvania
Contract No. F29601-67-C-0086

TECHNICAL REPORT NO. AFWL-TR-68-96

FOREWORD

This report was prepared by the University of Pittsburgh, Pittsburgh, Pennsylvania, under Contract No. F29601-67-C-0086. The research was performed under Program Element 61102H, Project 5710, Subtask 07.003, and was funded by the Defense Atomic Support Agency (DASA).

Inclusive dates of research were 30 June 1967 to 30 June 1968. The report was submitted 24 September 1968 by the AFWL Project Officer, Capt Joseph S. Greene, Jr. (WLRTH).

Information in this report is embargoed under the Department of State ITIARs. This report may be released to foreign governments by departments or agencies of the U. S. Government subject to approval of AFWL (WLRTH).

This technical report has been reviewed and is approved.

JOSEPH S. GREENE, JR.
Captain, USAF
Project Officer

TRUMAN L. FRANKLIN
Colonel, USAF
Chief, Theoretical Branch

CLAUDE K. STAMBAUGH
Colonel, USAF
Chief, Research Division

ABSTRACT

Three types of experiments were performed to study collision properties of ions in the energy range from approximately 50 keV to 2 MeV. The first study made measurements of the electron capture and loss cross sections of N^+, O^+, Xe^+, and U^+ in collision with N_2, O_2, Ar, and Ne. Results for stripping of electrons from the neutral atoms of the above ions were deduced from the data as well. The second study measured the cross sections for exciting the (0,0) transition of the first negative bands of N_2^+ at 3914Å on impact of Ba^+, Ba^{++}, Xe^+, O^+, N^+, and N_2^+ on N_2. In the third study an initial attempt was made to measure the cross section of electron-impact excitation of He^+ to the $n = 2$ state, wherein a fast beam of He^+ was passed through a space charge limited electron cloud and the 304Å photons were to be measured. While this novel approach has not yielded the desired cross section, the general approach of placing relative energy in the ion instead of in the electron when studying the interactions between ions and electrons appears to have considerable promise.

(Distribution Limitation Statement No. 2)

CONTENTS

ILLUSTRATIONS

TABLES

SECTION I

INTRODUCTION

The experimental program was originally planned to consist of four parts:

A. Measurement of electron capture and loss cross sections and ionization cross sections in collisions of heavy ions and atoms with atmospheric gases and certain rare gases;

B. Measurement of energy loss cross sections with the same collision partners;

C. Study of electron-ion collision processes in which the relative velocity was obtained by giving energy to the ions rather than to the electrons;

D. Study of excitation of radiation, and in particular the measurement of lifetimes of radiating states of heavy ion and atom species.

In all experiments the 2 MeV Van de Graaff accelerator provided by the Air Force Weapons Laboratory was to be used and emphasis was to be placed on heavy particle species other than the inert gases and alkalis.

During the interim between the writing of the proposal and the commencement of the actual research, several exigencies became apparent, which justified some modifications of emphasis in the program, and these were made accordingly. In Item A, for example, it became clear that data on O^+ and N^+ were needed more urgently than on some of the heavier particles originally planned and these substitutions were made. While it had been planned to measure ionization cross sections concurrently with the measurements of the capture and loss cross sections, it became evident that a greater need apparently existed for the measurement of optical excitation cross sections (particularly for 3914$\mathring{A}$ radiation from N_2^+) and these concurrent excitation measurements replaced the ionization measurements. Section II describes the electron capture and loss cross section measurements.

No work was done on Item B, which seemed to be of lower priority than the measurements actually performed.

Item C was undertaken with the goal of developing a new experimental approach to the experimental study of electron-ion collision processes. The technique places the relative kinetic energy between the collision partners in the ion rather than in the electron and thus attempts to avoid electron-beam-generated noise, which is an enormous problem in more conventional approaches to this area of study. In order to have a finite problem around which to develop the approach, the electron impact excitation of He^+ to cause radiation at 304Å was chosen because of its potential importance to the development of theory of electron-ion processes.

Section III describes the work of Item C.

Item D was originally intended to concentrate on measuring the lifetimes of certain radiating ionic states by using the beam-foil approach. However, because of interest in the excitation of the 3914Å radiation in heavy particle collisions with N_2, this portion of the program has been concerned exclusively with the measurement of these excitation cross sections, which are summarized in Section IV.

SECTION II

ELECTRON CAPTURE AND LOSS CROSS SECTION MEASUREMENTS

1. Theory of the Experiments

When a fast particle with i positive charges, A^{i+}, collides with a stationary neutral target particle, B, the reaction can be represented by

$$A^{i+} + B \rightarrow A^{j+} + B^{n+} + (j + n - i)e \tag{1}$$

and the cross section can be designated by Q_{ij}^{0n}. The capture and loss cross sections are defined by

$$\sigma_{ij} = \sum_{n} Q_{ij}^{0n} \tag{2}$$

and represent the total cross section for the fast particle changing charge from i+ to j+, irrespective of the change of charge state of the originally neutral slow target particle.

Measurements of the capture and loss cross sections are made by analyzing the charge state of the fast particle beam emerging from the region of collisions with the target gas. By designating F_m as the fraction of the fast beam, which has the charge m+, one can write

$$\frac{dF_m}{d\pi} = -q_m F_m + \sum_{j \neq m} \sigma_{jm} F_j \tag{3}$$

where $q_m = \sum_{k \neq m} \sigma_{mk}$ and $\pi = \int n(x)dx$, the integral of the target gas number density, n(x), over distance through the target gas. Since the geometry is fixed, changes in π through changes in target gas number density and accompanying changes in the fast particle beam charge constituents give the basic data from which the cross sections are obtained.

If one starts out with a beam in a well-defined charge state, in the limit of low π, Eq. (3) solves to give

$$F_i = 1 - q_i\pi \tag{4a}$$

$$F_j = \sigma_{ij}\pi \tag{4b}$$

to first order in π and it is Eq. (4b) that is used to obtain the capture and loss cross sections where $i \neq 0$. The number density is varied (by varying the pressure in the target gas cell) and the slope of the curve of F_j vs. π in the region of π where F is linearly increasing gives the cross section immediately.

For electron loss cross sections from neutrals, the present experiments relied upon finding a value of π at which $dF_0/d\pi$ became zero, in which case the appropriate one of Eq. (3) becomes

$$\frac{dF_0}{dn} = 0 = -q_0F_0 + \sigma_{10}F_1 + \sigma_{20}F_2 + \ldots \tag{5}$$

In the energy range of these experiments, the cross section for multiple electron capture is very much less than for single electron capture, and provided that F_1 is not small compared to F_2, F_3, etc., all terms except the first two can be neglected to good approximation, yielding

$$q_0 \cong \sigma_{10}\frac{F_1}{F_0} \tag{6}$$

By using primary ions with a single charge, this latter condition was found to be met, thus justifying the use of Eq. (6) to estimate q_0. In general at the lower energies q_0 becomes equal to σ_{01} but at the higher energies, multiple stripping begins to enter. In the present experiments only q_0 was determined by using Eq. (6).

2. Experimental Considerations

The experimental approach has been described in previous reports (Ref. 1, 2, and 3) and will not be described in detail here. In general a beam of ions is produced in an ion source, the beam is

accelerated in the Van de Graaff accelerator, enters the cell containing the target gas, and is analyzed after emergence by separating the variously charged species by means of deflection in a transverse electrostatic field.

In most experiments, a magnetic analysis of the beam is made after acceleration in order to select particles of the desired e/m for injection into the gas cell. However, in the case of very heavy ions travelling at MeV energies, the magnets and drift distances become inconveniently large, and an alternative procedure was used to obtain purity of the primary beam in the present experiments. First, ion species selection was made in the head of the accelerator by passing the ions through a small quadrupole mass filter before they had obtained appreciable energy. The selected ions were then accelerated. Since considerable distance is involved in the accelerator tube, charge capture and loss processes will occur during acceleration thus changing the charge states of the desired chemical species of ion and also forming some background gas ions that are accelerated along with the desired ions. Since the background gas ions will be formed all along the length of the acceleration tube, their energy will be less than that of the desired primary ion; similarly if a primary ion changes charge along the acceleration tube, it too will arrive at the end of the tube with a different kinetic energy than the desired ion will have. By performing an energy analysis after acceleration, both types of unwanted ions can be removed from the primary ion beam. The beam was purified by deflection in a transverse electrostatic field, the primary desired ion beam being deflected by 2° some 60 cm before the collision chamber.

A second change in the experimental methods used in the present experiments was the use of an open electron multiplier to detect the ions. Since at the energies of these experiments the secondary electron emission coefficients are independent of the charge state

of the ion striking the first dynode, comparison of the observed analyzed product of the fast-particle signals gave immediately the relative fractions of fast particles in the various charge states.

As in the experiments performed previously at the University of Pittsburgh (Ref. 1, 2, and 3), the fast-particle detector could be rotated about a center under the interaction volume and the transverse analyzing field could be varied, thus minimizing systematic errors that could occur if either degree of freedom were removed. Also, as in our previous experiments, the gas cell was constructed with a circular entrance aperture (diameter 1 mm) and an exit "half-slit" of dimensions 2 mm × 5 mm. By orienting the long axis of this slit parallel to the direction of travel of the rotating detector, it was possible to examine the angular spreading of each product ion beam and thereby select an aperture size before the detector sufficiently large to ensure no discrimination against ions that underwent angular deflections during the electron capture or loss collisions.

Two minor changes were made in the present measurements; first, the collision chamber was located in the final stage of the vacuum system rather than in an intermediate chamber as previously. This change was made in order to accommodate the lenses, interference filter and photomultiplier that were appended to the collision chamber to allow its being used to measure excitation cross sections as well as the capture and loss cross sections. The second change was the use of the more conventional dc measuring technique rather than the ac lock-in technique described in References 1, 2, and 3. This was found to be more convenient because of the additional signal gain afforded by the open electron multiplier detector.

The ion sources used for the production of metal ions were those previously described (Ref. 1 and 3). For the gaseous ions, He^+, N^+, O^+, Xe^+, etc., an unusually efficient electron impact ionizer, designed for neutral atomic beam detection, was modified and installed

in the head of the Van de Graaff machine. Figure 1 shows a schematic of this source and shows the quadrupole mass filter for ion selection, discussed at the beginning of this section, as well. The ionizer operates by electrons emitted from four filaments surrounding a cylindrical cage grid, entering the grid enclosure, and ionizing neutral gas there. The electron currents graze very closely to the extraction lens, establish a weak quasi-plasma in the extraction lens aperture, from which the ions are drawn.

At very low source pressures this source used in conjunction with the mass filter tuned for a mass resolution of 40 will produce currents of approximately 10 mA of ions per torr. In practice, with the apertures chosen in the present source gas leaking from the source into the mass filter region (where the high fields can set up a radiofrequency discharge) the source gas pressure had to be kept below about 10^{-4} torr, giving maximum resolved ion currents of about 10^{-6} amperes. This was more than adequate for all the capture and loss cross section measurements to be performed and no effort was made to optimize the operation of the ion source and mass filter. The ion source uses about 25 watts filament power with an electron emission current of 50 mA.

Pressure measurements, from which the number densities required in Eq. (4b) were obtained were made by using a differential capacitance manometer* operating between the collision chamber and the vacuum of the main chamber. The procedure in taking measurements was to fill the collision chamber and a gas reservoir to a given initial pressure after which the flow of gas into the system was cut off. As the gas escaped out of the apertures in the collision chamber, the pressure slowly diminished. The manometer reading was put on the X axis of an X-Y recorder and

*MKS Baratron

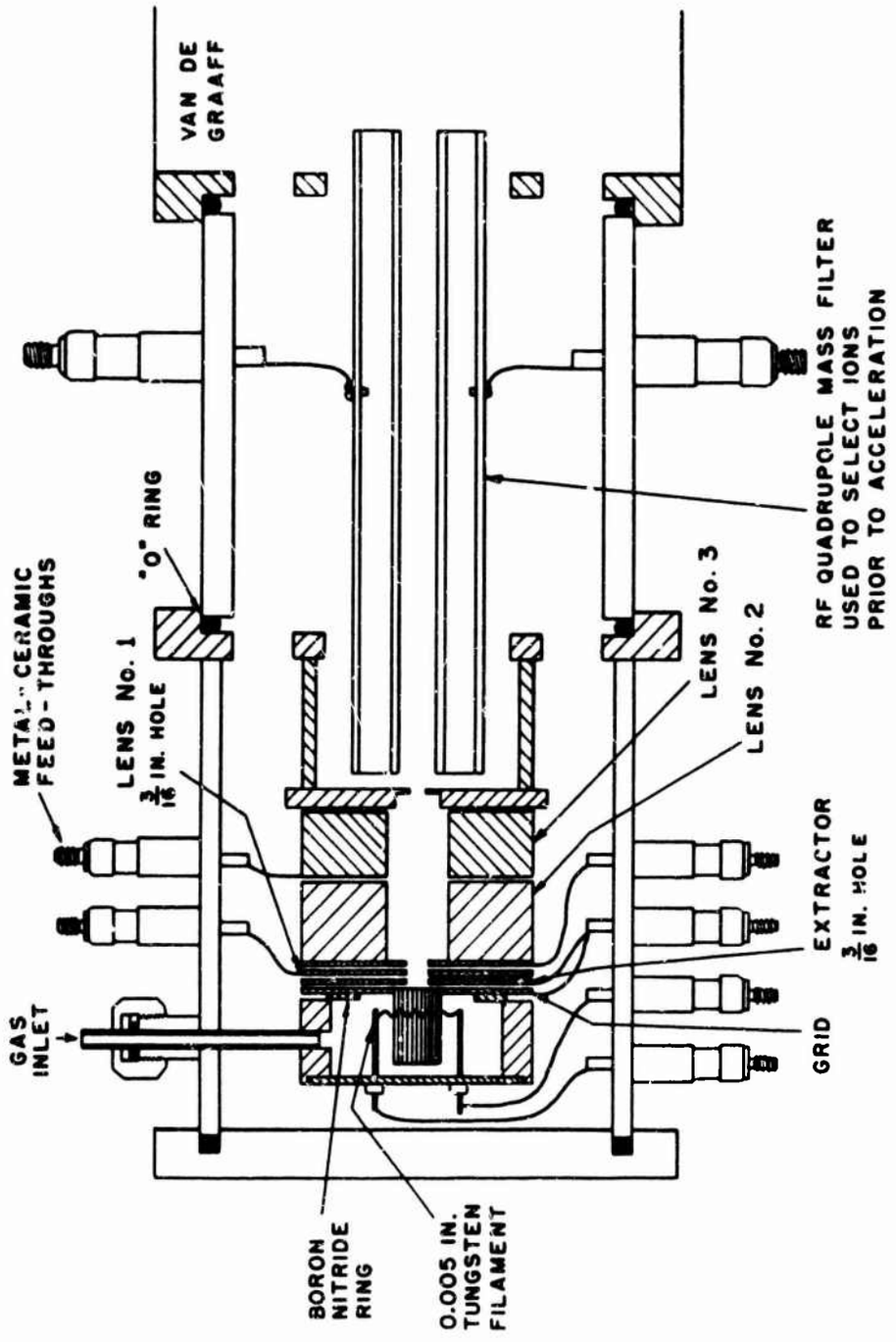

Figure 1. Source for Production of Gaseous Ions

the signal on the Y axis, so that a plot of signal vs. pressure was obtained immediately, the slopes of which gave the cross section of Eq. (4b).

The manometer was calibrated at pressures of the order of 10^{-3} torr and higher against a McLeod gauge that was dry-ice trapped against the Ishii-Nakayama effect. Linearity of the manometer from 10^{-4} to 10^{-3} torr was established by comparison of its readings against those of an ionization gauge.

3. Results

The principal new results on capture and loss cross sections are given in Figures 2 through 17.

Figures 2 through 5 show results of N^+ ions colliding with the target gases N_2, O_2, Ar, and Ne. The only other data of which we are aware against which to compare the present measurements are those of the group of V. S. Nikolaev on the target gases N_2 and Ar. Figures 2 and 4 show these data (Ref. 4, 5, and 6) along with the present results. The agreement between the two sets of results is generally quite satisfactory. A comparison of the experimental arrangements would suggest that the higher stripping cross sections σ_{13} and σ_{14} should be higher in our experiments since the Russians' arrangement would be expected to discriminate slightly against particles that undergo small-angle deflections in the collisions. It is not clear why the agreement on σ_{12} in $N^+ + N_2$ collisions is not better than it is, although a 30 percent discrepancy is perhaps not too serious in this type of measurement.

Figures 6 through 9 summarize the cross sections for O^+ ions in the same four target gases. We are not aware of any other data against which these results can be compared.

Figures 10 through 13 show the cross sections for Xe^+ ions in

N_2, O_2, Ar, and Ne. It is interesting to note that in Neon in addition to σ_{10} being rather small and peaking at a high velocity (which is generally to be expected on the basis of the adiabatic theory of charge transfer), the neutral stripping cross section q_0 is noticeably smaller for Ne than for the other gases, a point that is not so evident in the case of the lighter fast particles.

Figures 14 through 17 summarize the situation when the primary fast particles are Uranium atoms and ions. Uranium data with N_2, O_2, and Ar target gases were taken two years ago when we were using a 400 keV Van de Graaff accelerator and those results were presented in Reference 1. The newer data were taken to extend the energy range up to a full 2 MeV (velocity = 1.3×10^8 cm/sec), and to add Ne as a target gas.

As is evident from the figures, the newer results for the stripping cross sections q_0 and σ_{12} are in very good agreement with the older results at energies where the two sets of data overlap. In less satisfactory agreement are the capture cross sections σ_{10}. While the magnitude of these cross sections is in moderately good agreement for N_2 and Ar, it is disconcerting to note difference in details of the curves, particularly the apparent absence of "structure" in the newer data using Ar as the target. Disagreement by a factor of 2 in the case of σ_{10} for U^+ on O_2 between the older and newer data is particularly disturbing.

No less disturbing is the finding that for the higher stripping cross sections, σ_{13} and σ_{14}, the newer data are uniformly higher than the older results, when the target gases were N_2 and Ar. The discrepancy suggests that in the older data, despite what we thought were adequate precautions, not all of the higher stripped ions were being detected and that the apertures were not large enough to intercept the ions that had undergone small-angle collisions in the higher electron loss collisions.

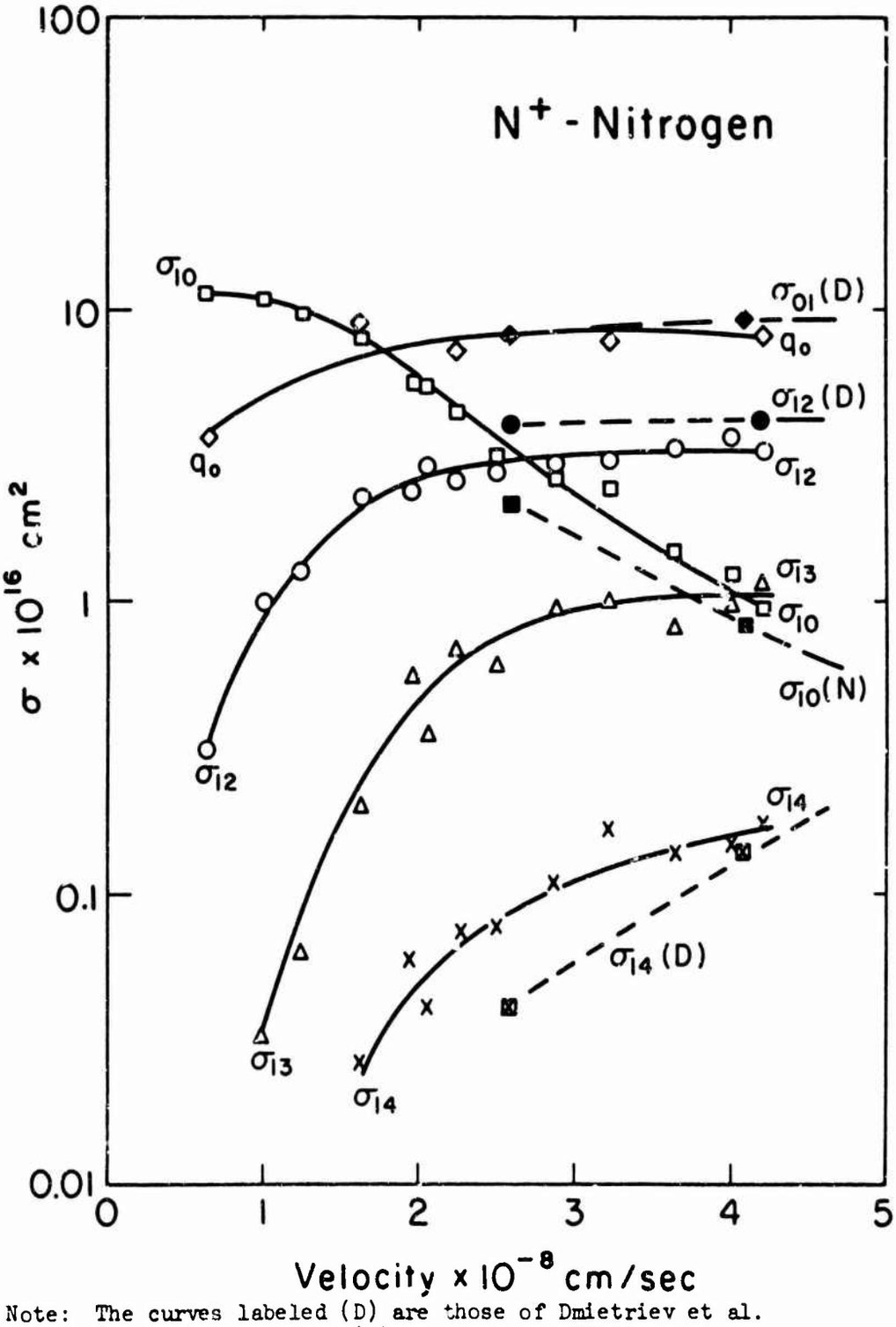

Note: The curves labeled (D) are those of Dmietriev et al. (Refs. 4 and 5) and (N) are those of Nikolaev et al. (Ref. 6).

Figure 2. Electron Capture and Loss Cross Sections of N^+ in N_2

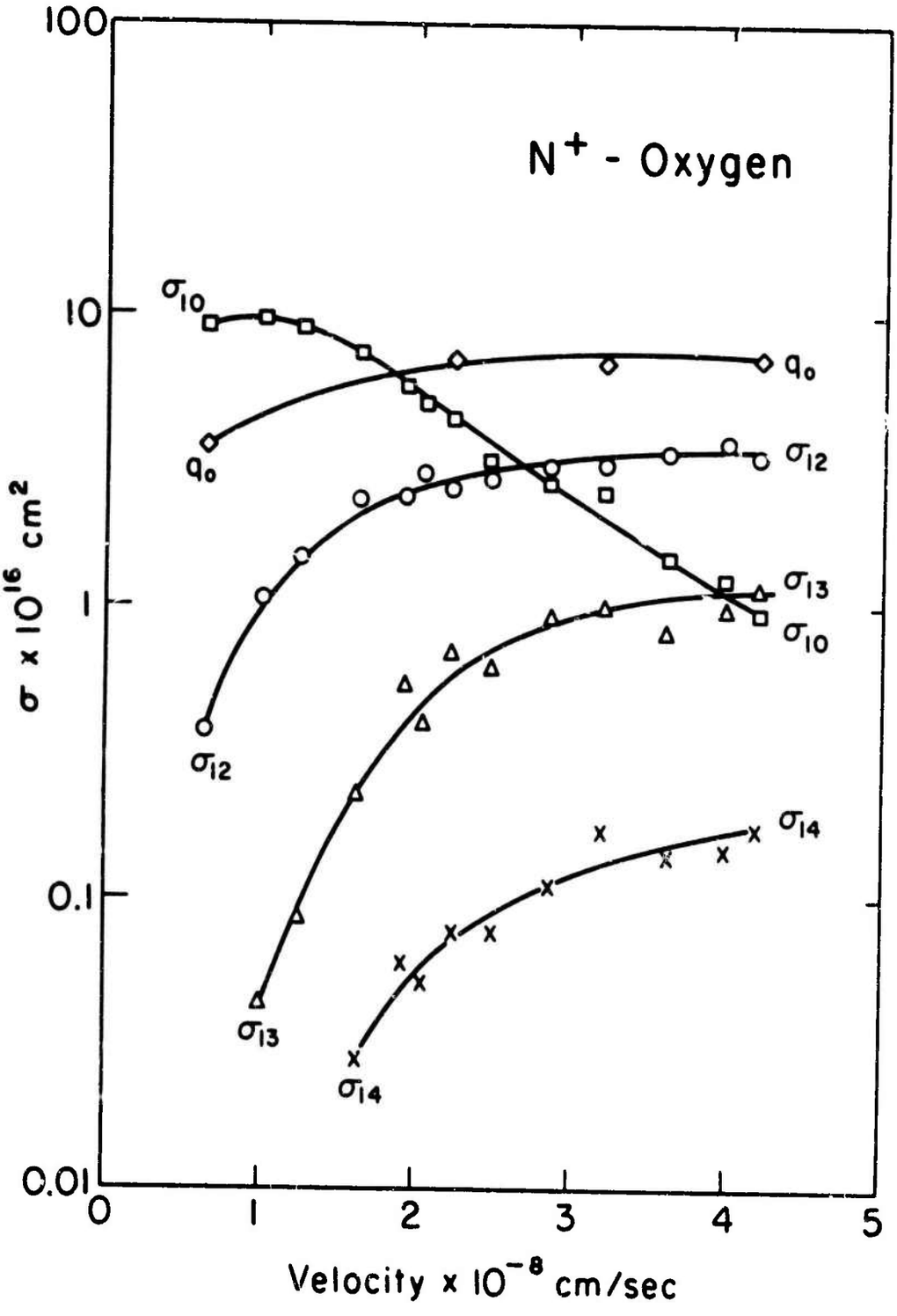

Figure 3: Electron Capture and Loss Cross Sections of N^+ in O_2

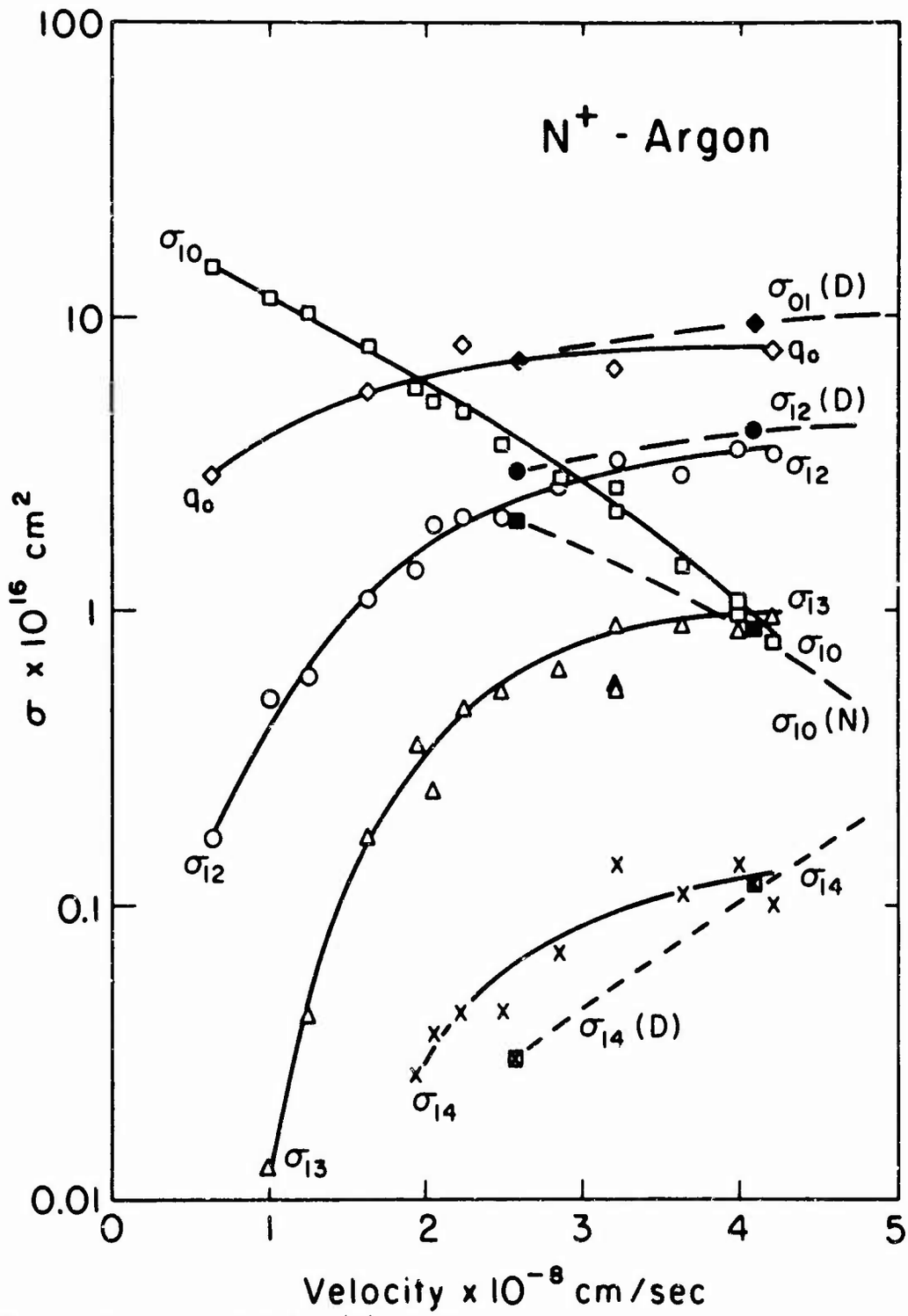

Note: The curves labeled (D) are those of Dmietriev et al. (Refs. 4 and 5) and (N) are those of Nikolaev et al. (Ref. 6).

Figure 4. Electron Capture and Loss Cross Sections of N^+ in Ar

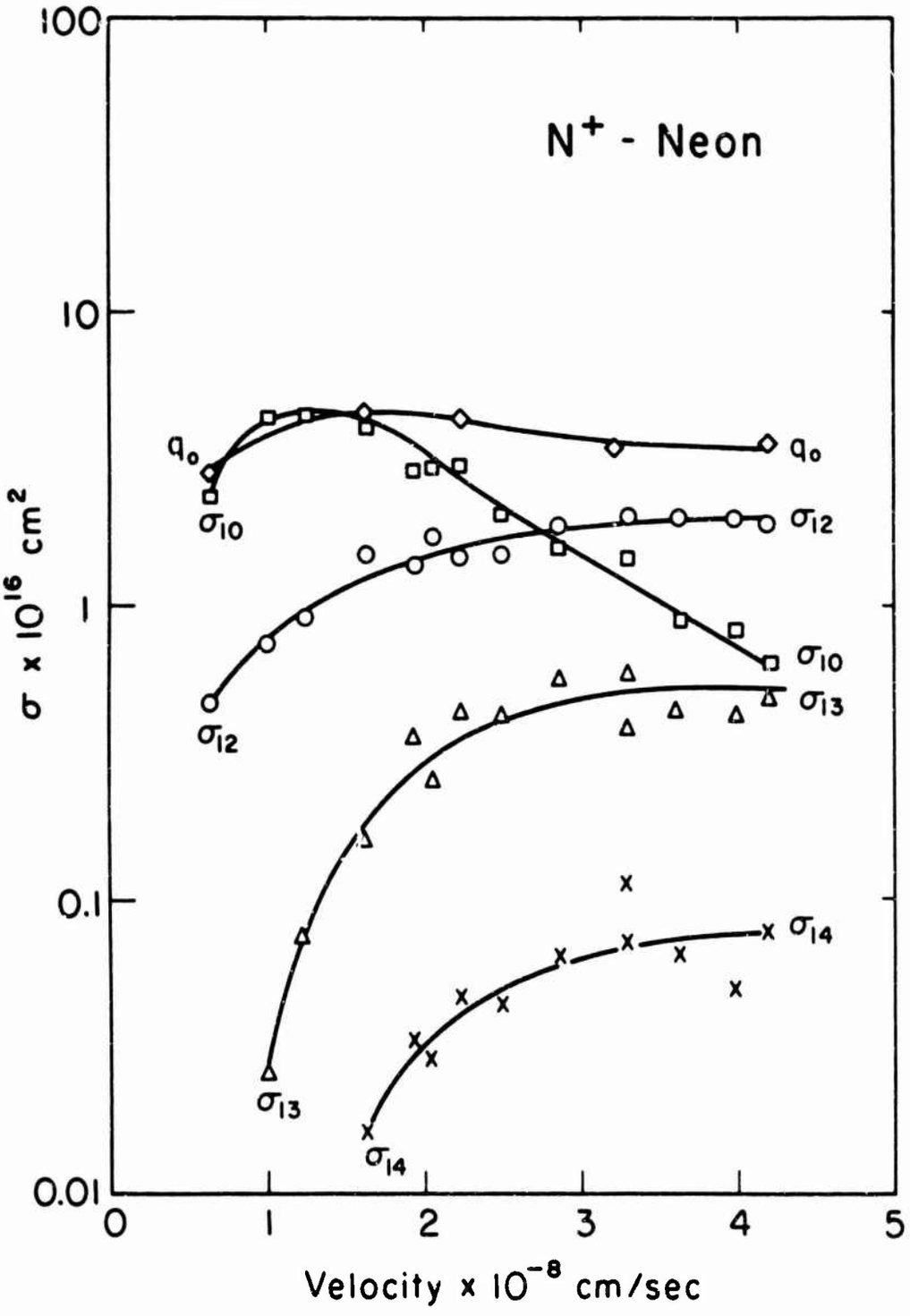

Figure 5. Electron Capture and Loss Cross Sections of N^+ in Ne

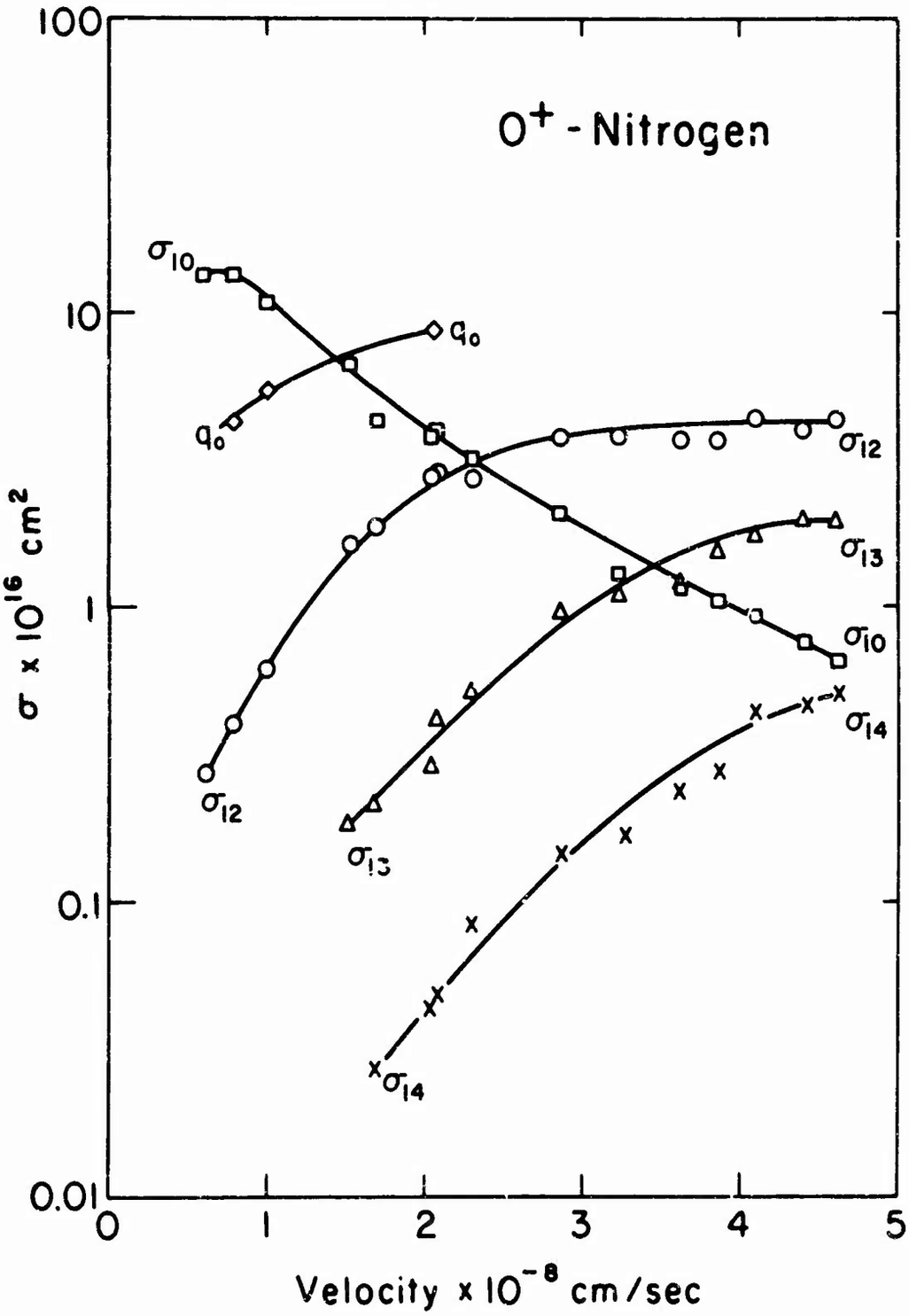

Figure 6. Electron Capture and Loss Cross Sections of O^+ in N_2

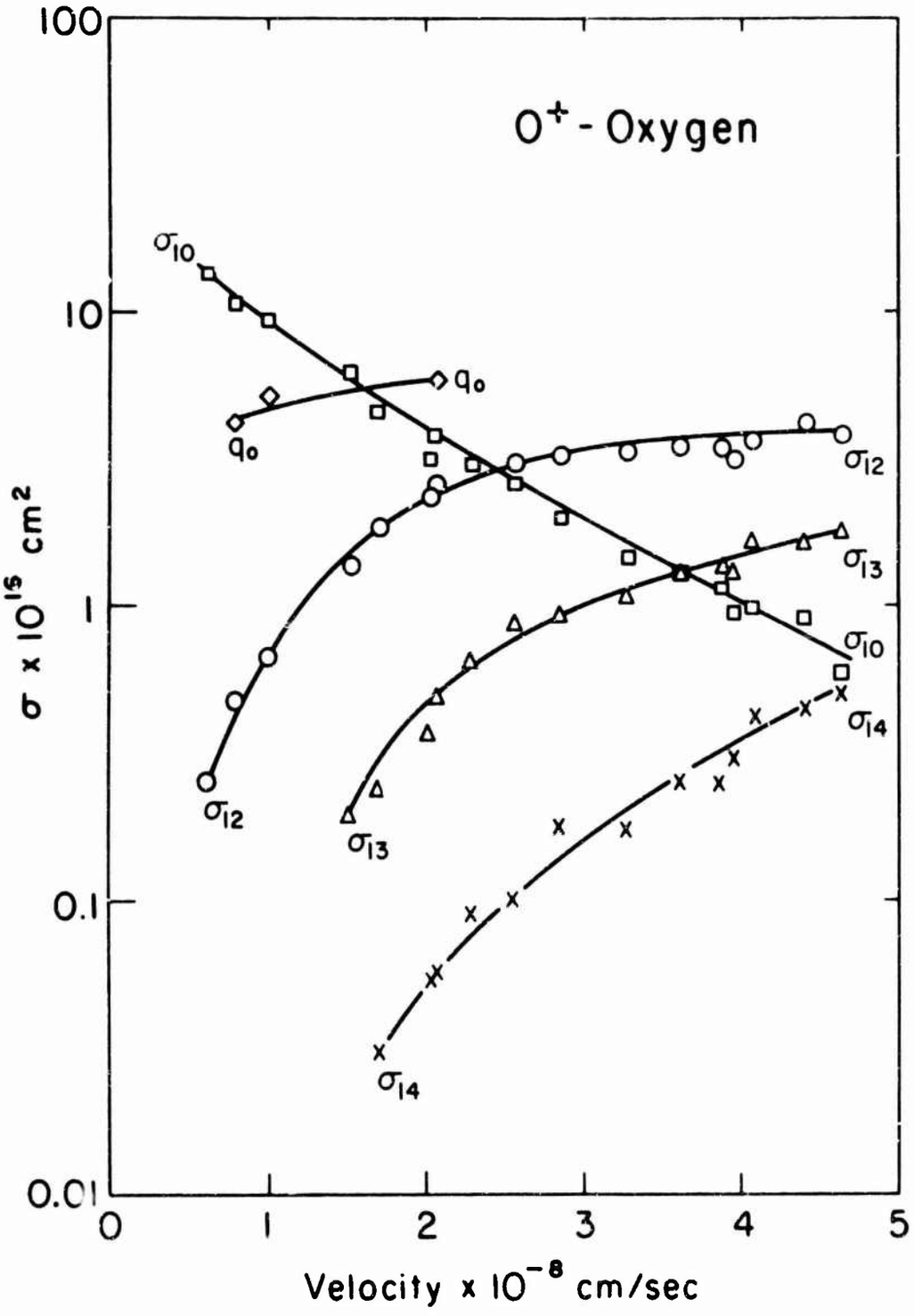

Figure 7. Electron Capture and Loss Cross Sections of O^+ in O_2

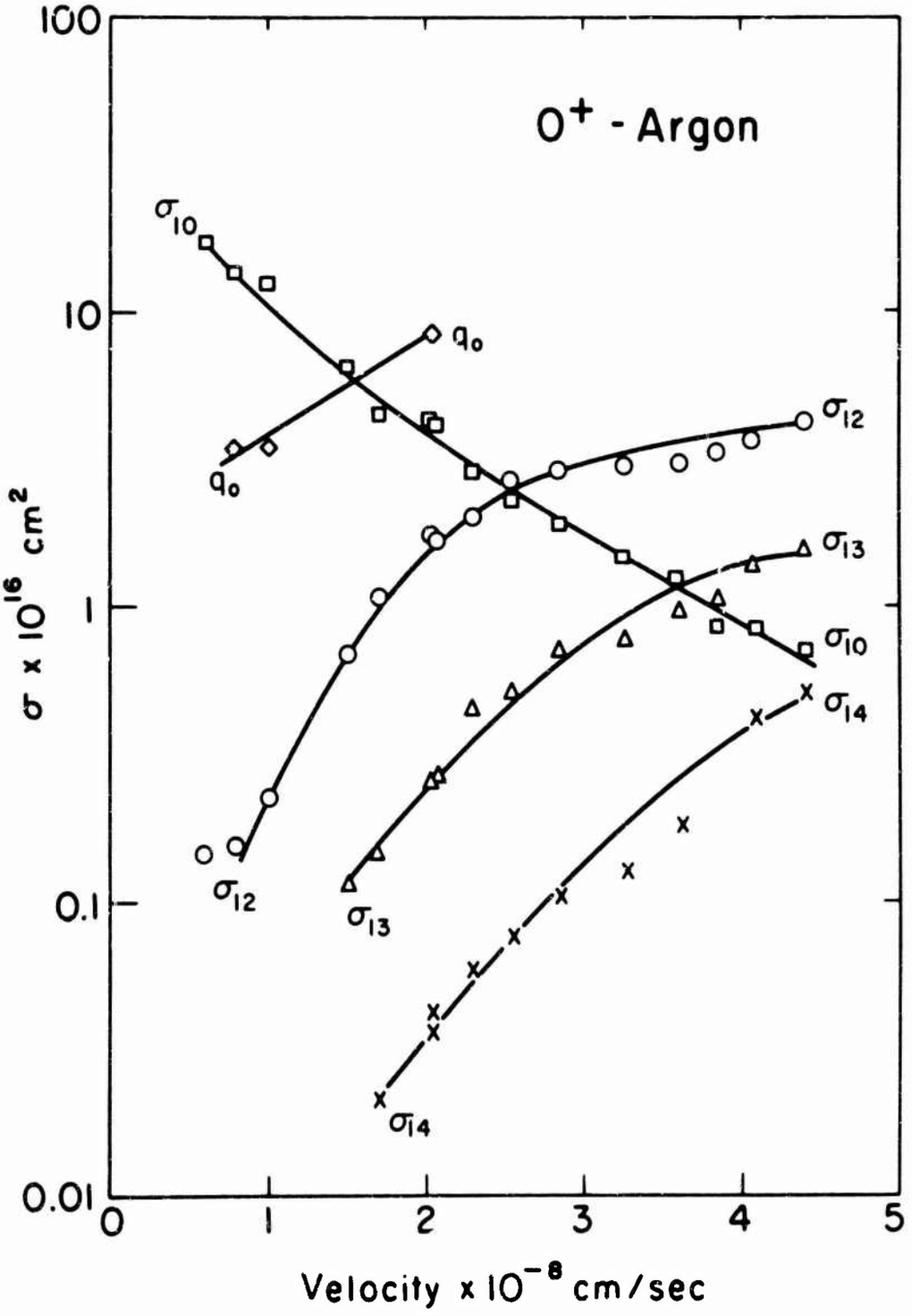

Figure 8. Electron Capture and Loss Cross Sections of O^+ in Ar

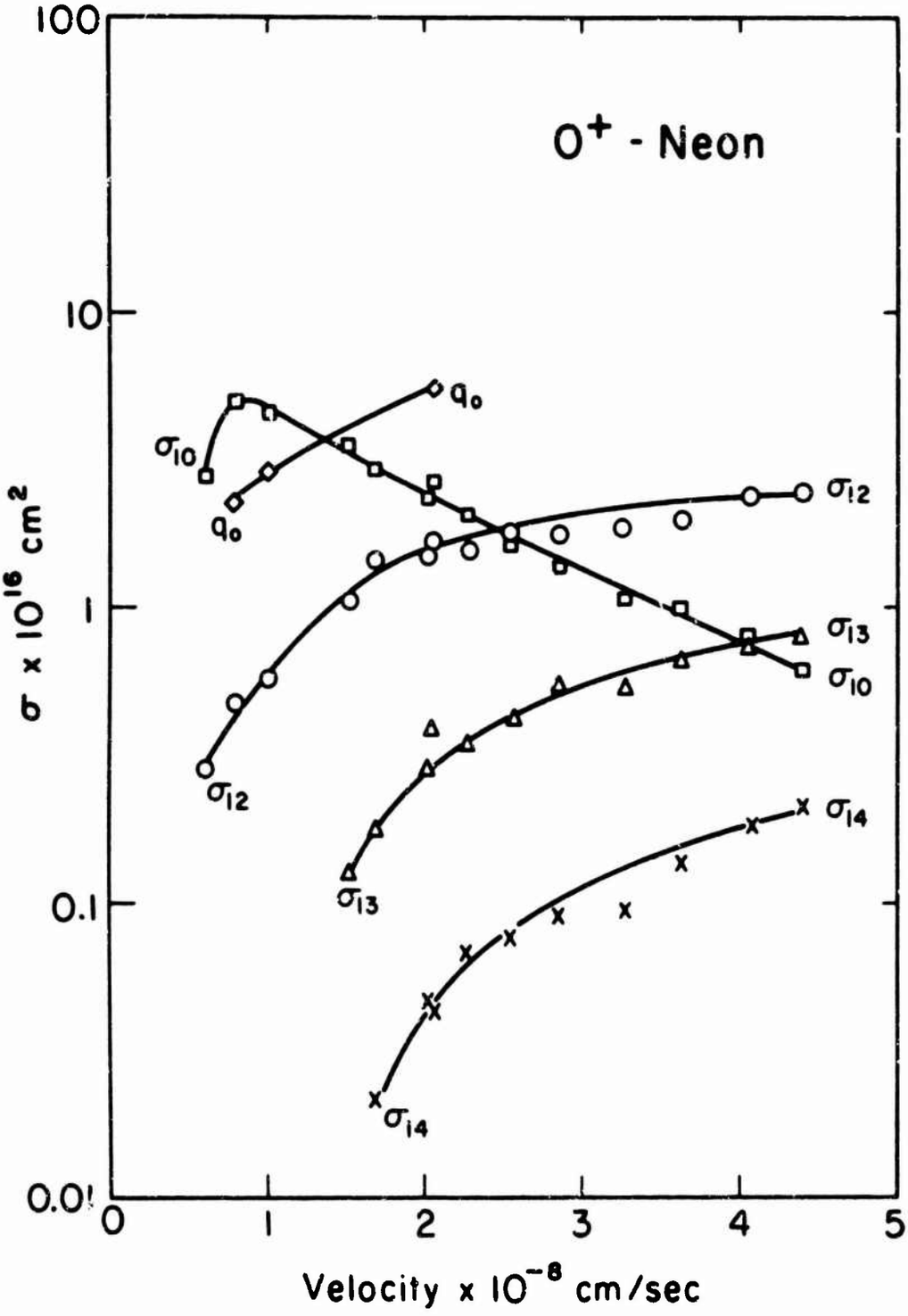

Figure 9. Electron Capture and Loss Cross Sections of O^+ in Ne

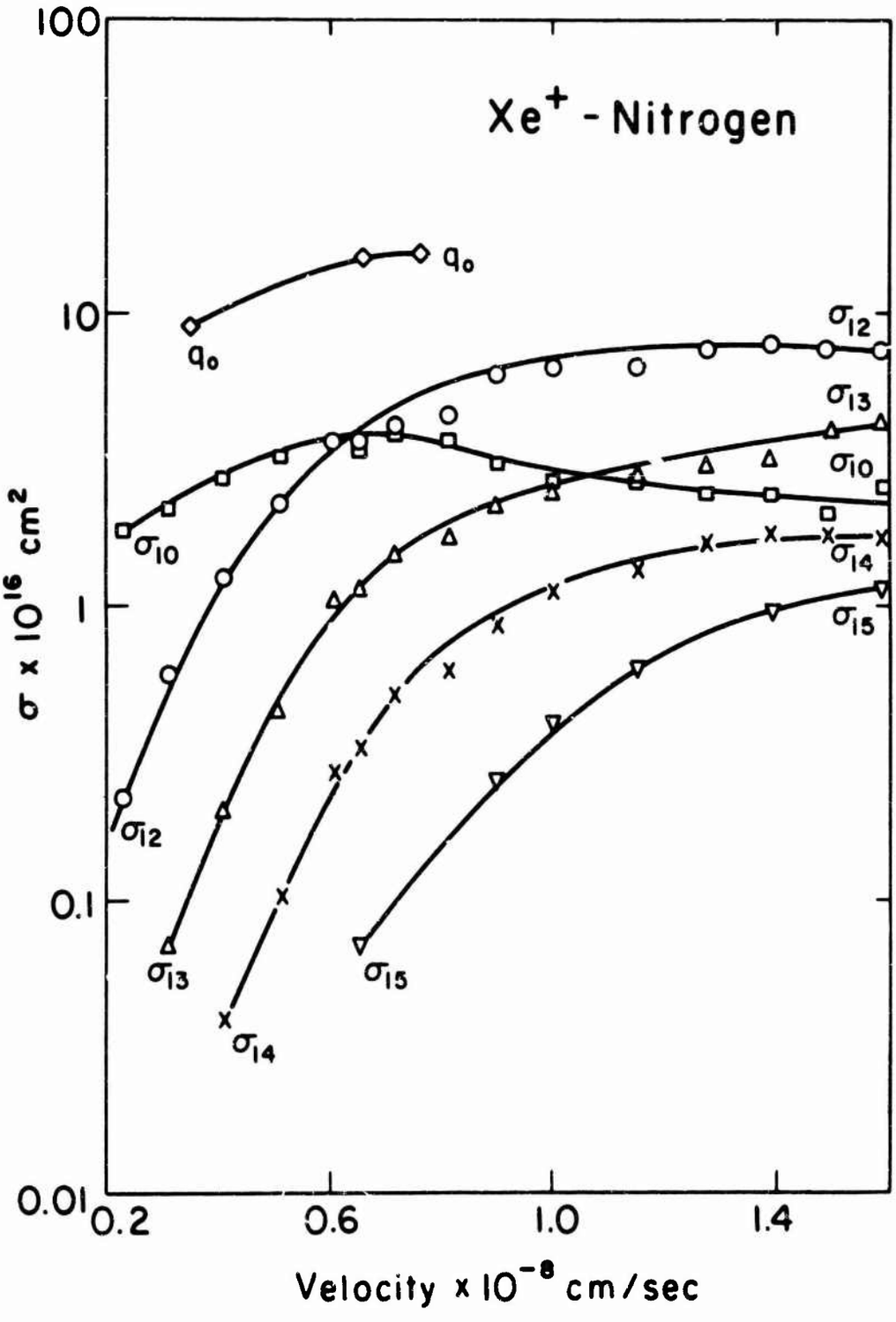

Figure 10. Electron Capture and Loss Cross Sections of Xe^+ in N_2

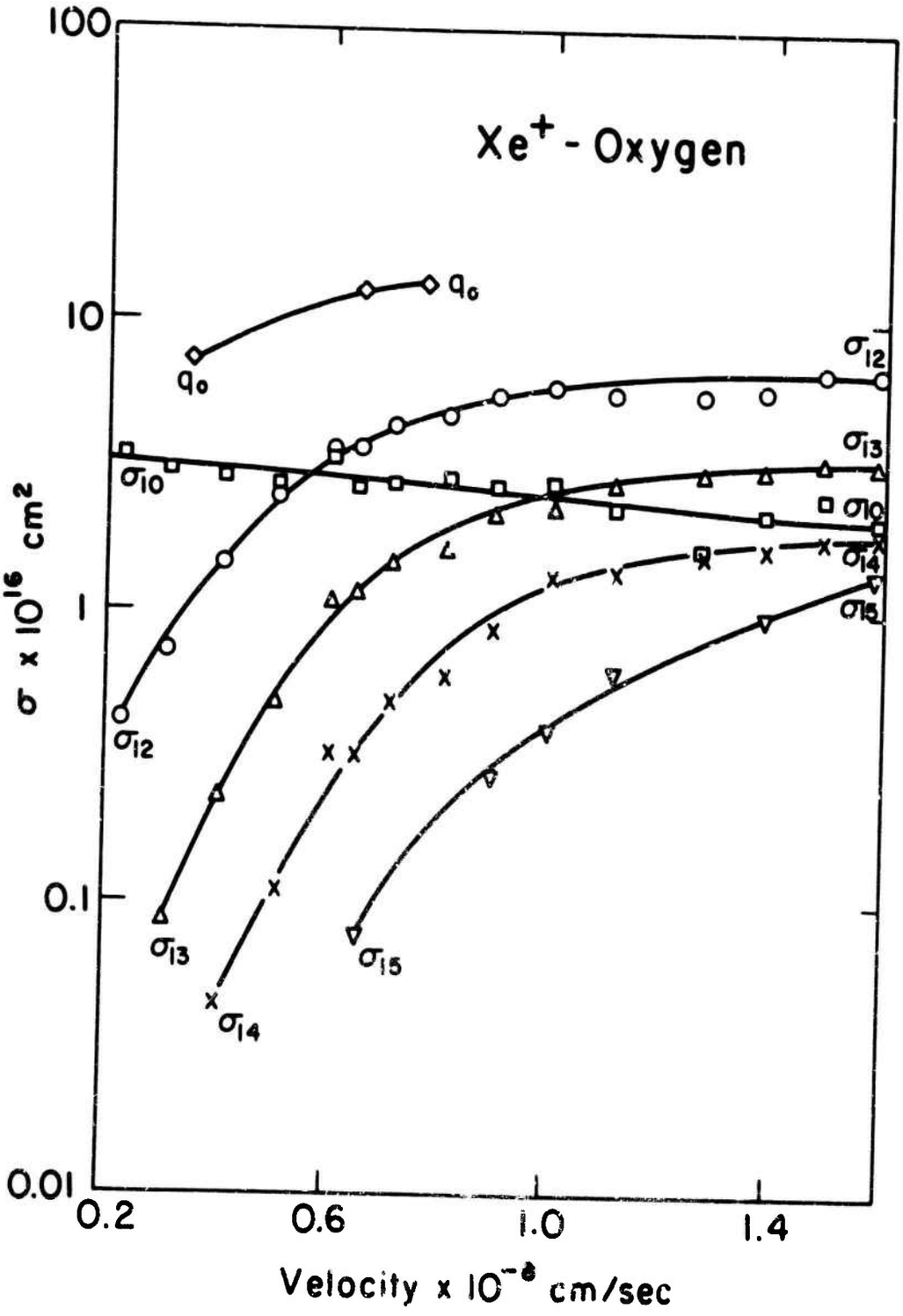

Figure 11. Electron Capture and Loss Cross Sections of Xe^+ in O_2

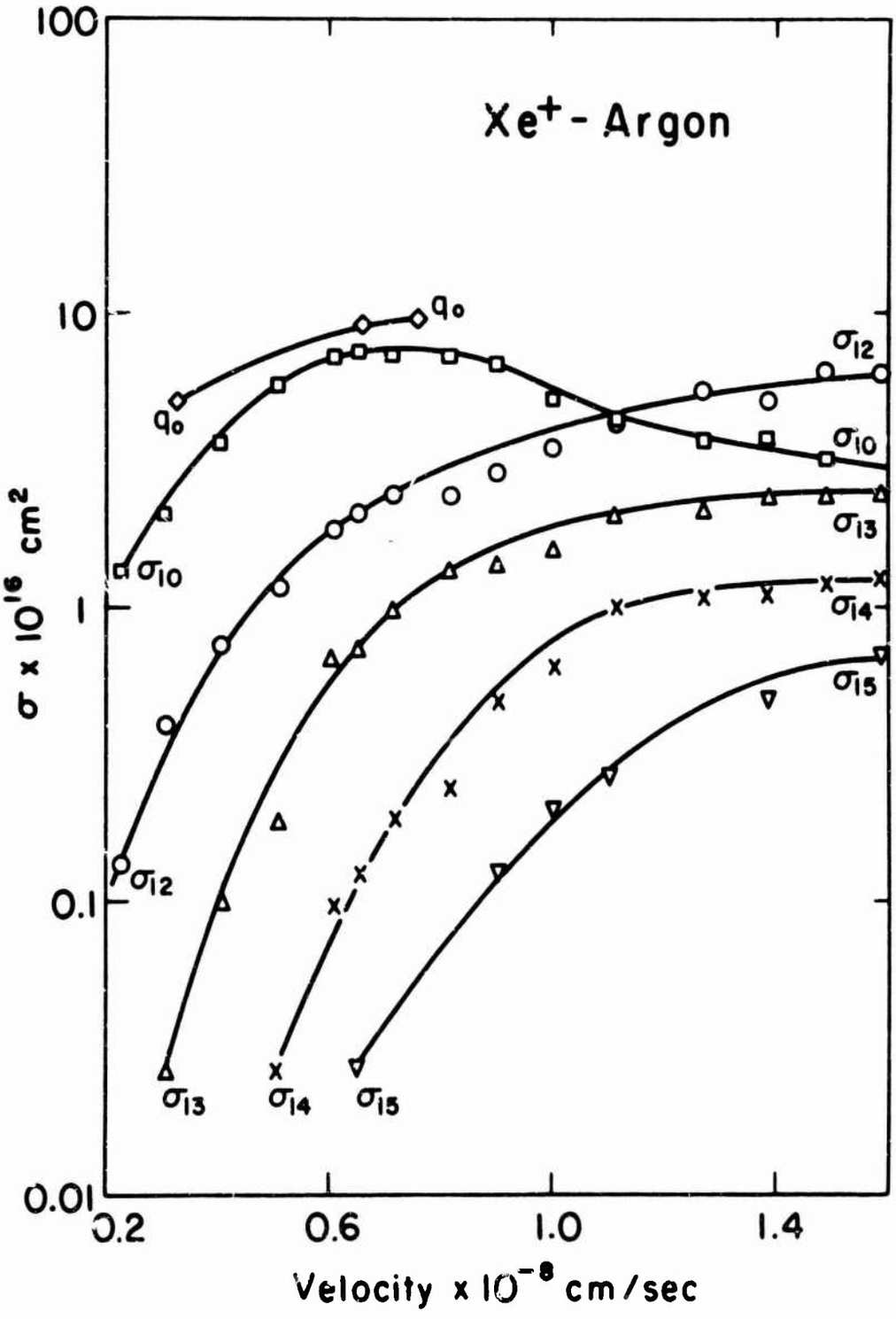

Figure 12. Electron Capture and Loss Cross Sections of Xe^+ in Ar

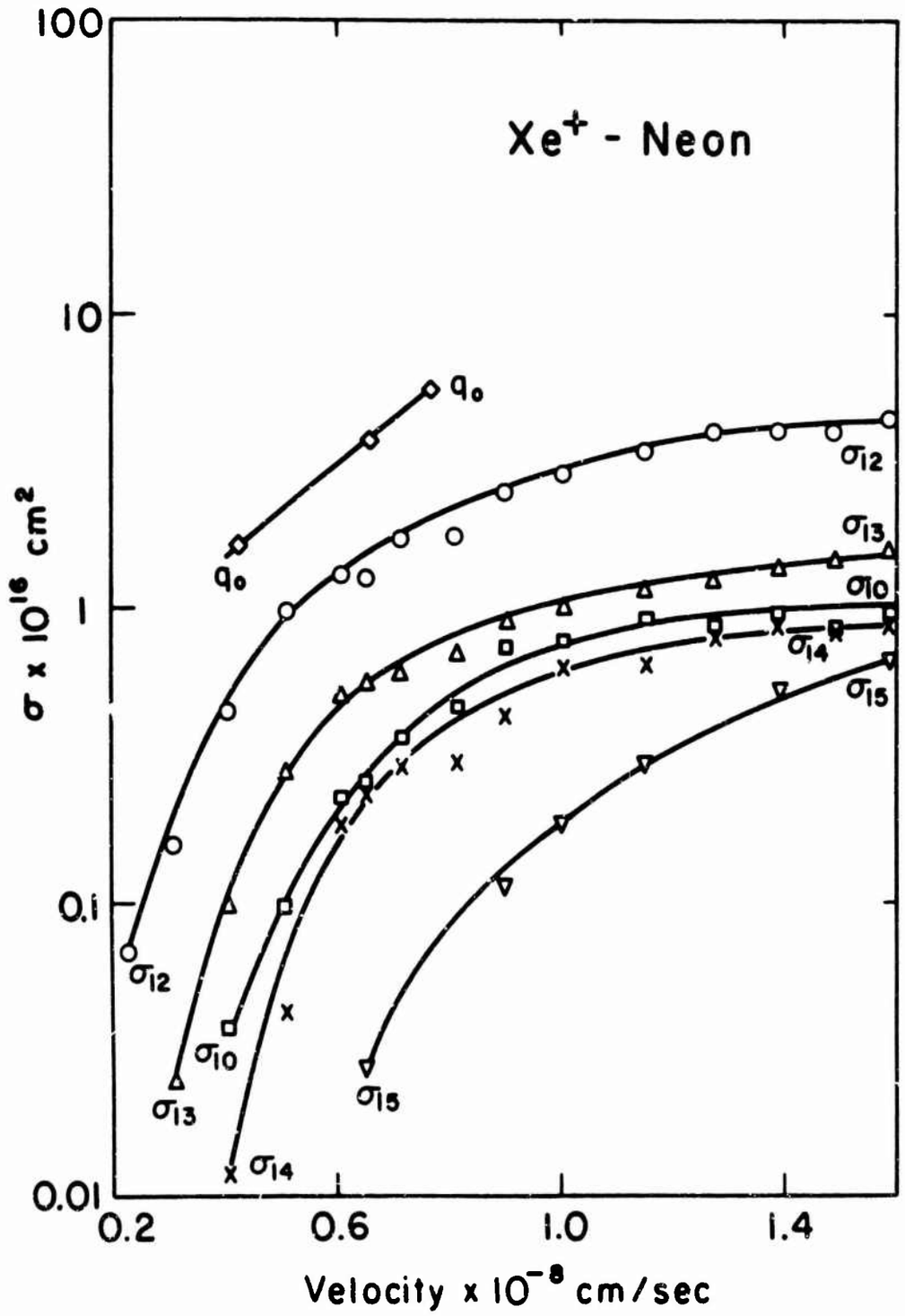

Figure 13. Electron Capture and Loss Cross Sections of Xe^+ in Ne

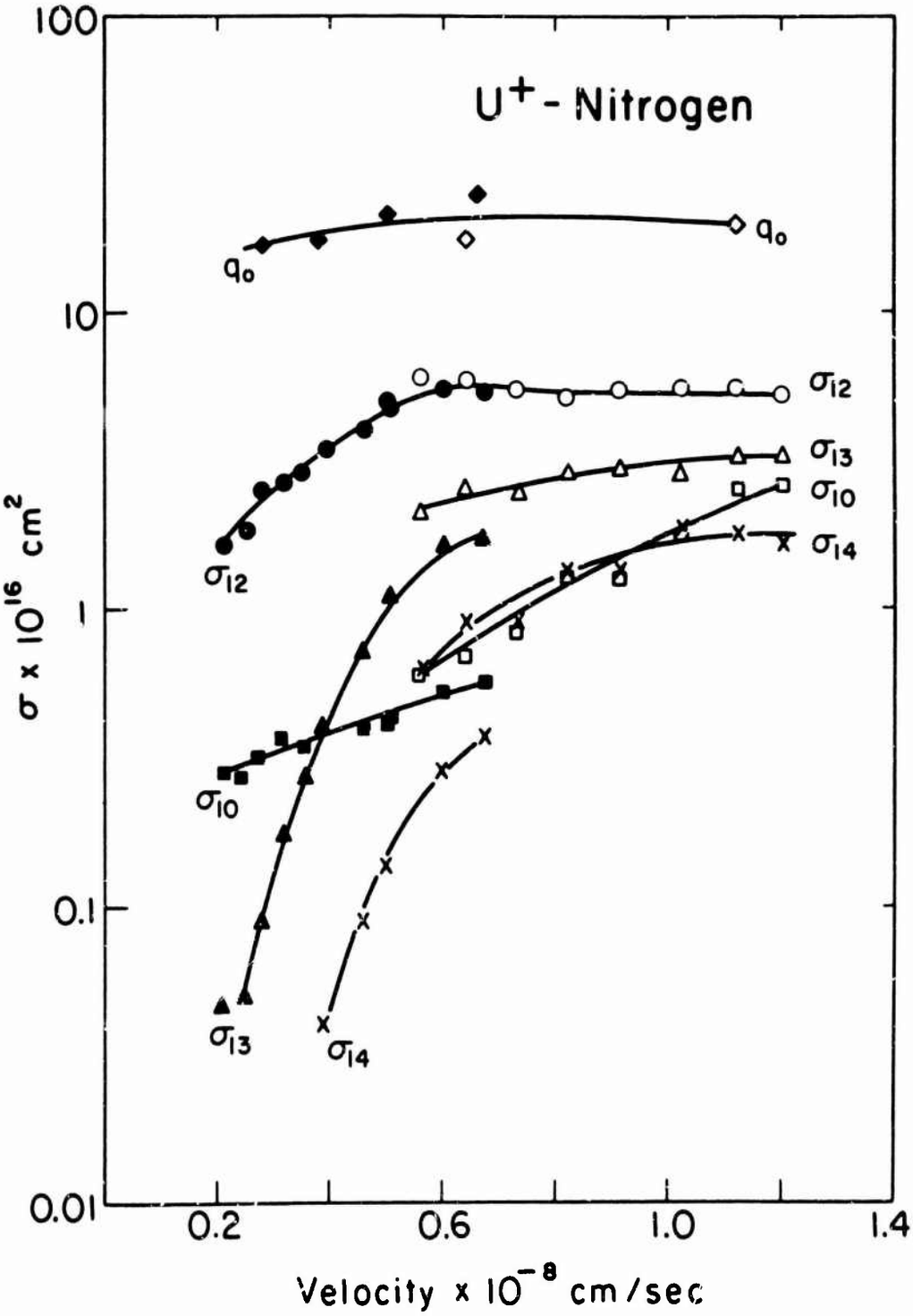

Note: Data taken earlier (Ref. 1) at the lower energies are indicated by solid data points and the most recent data by the open data points.

Figure 14. Electron Capture and Loss Cross Sections of U^{+} in N_2

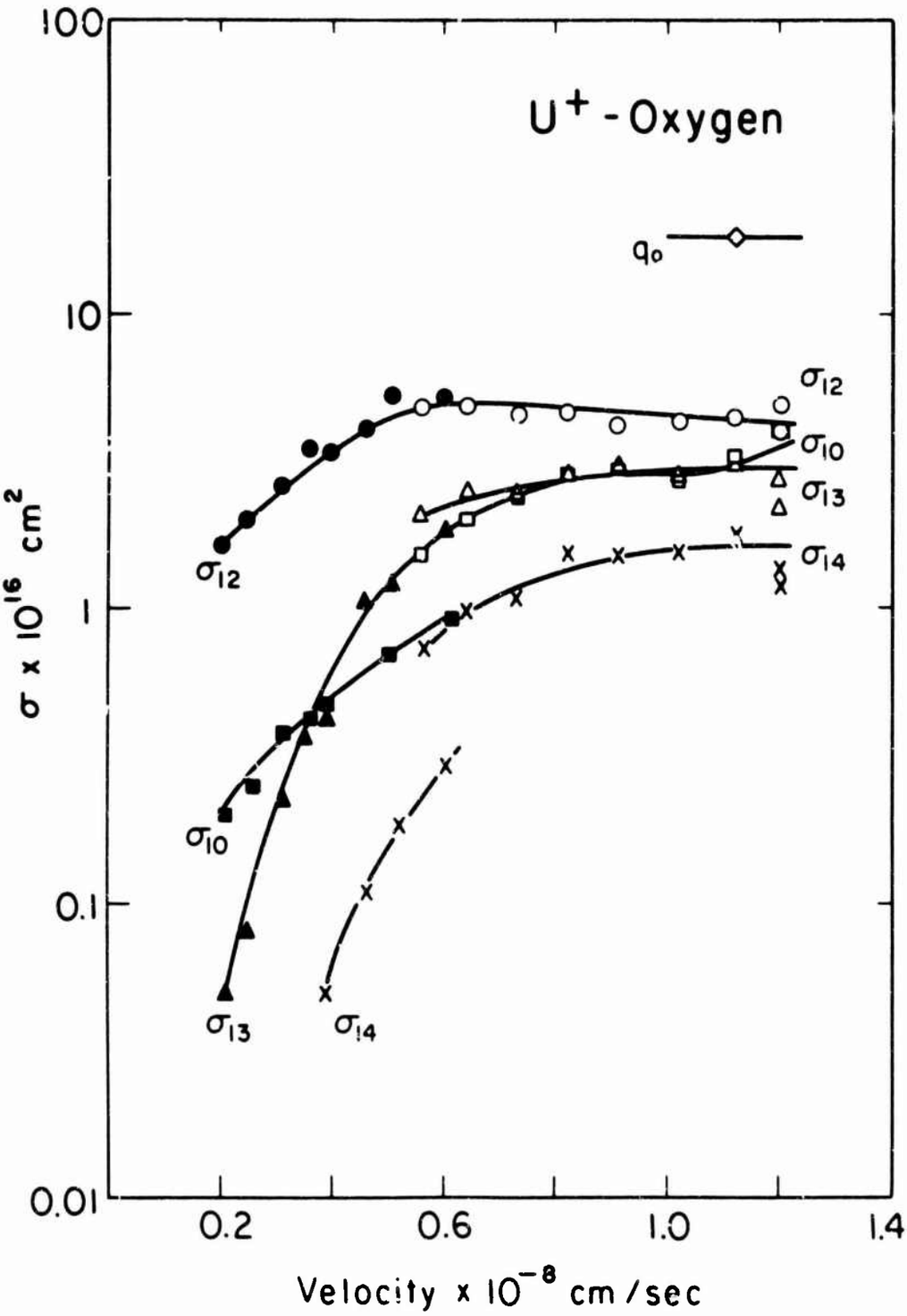

Note: Data taken earlier (Ref. 1) at the lower energies are indicated by solid data points and the most recent data by the open data points.

Figure 15. Electron Capture and Loss Cross Sections of U^+ in O_2

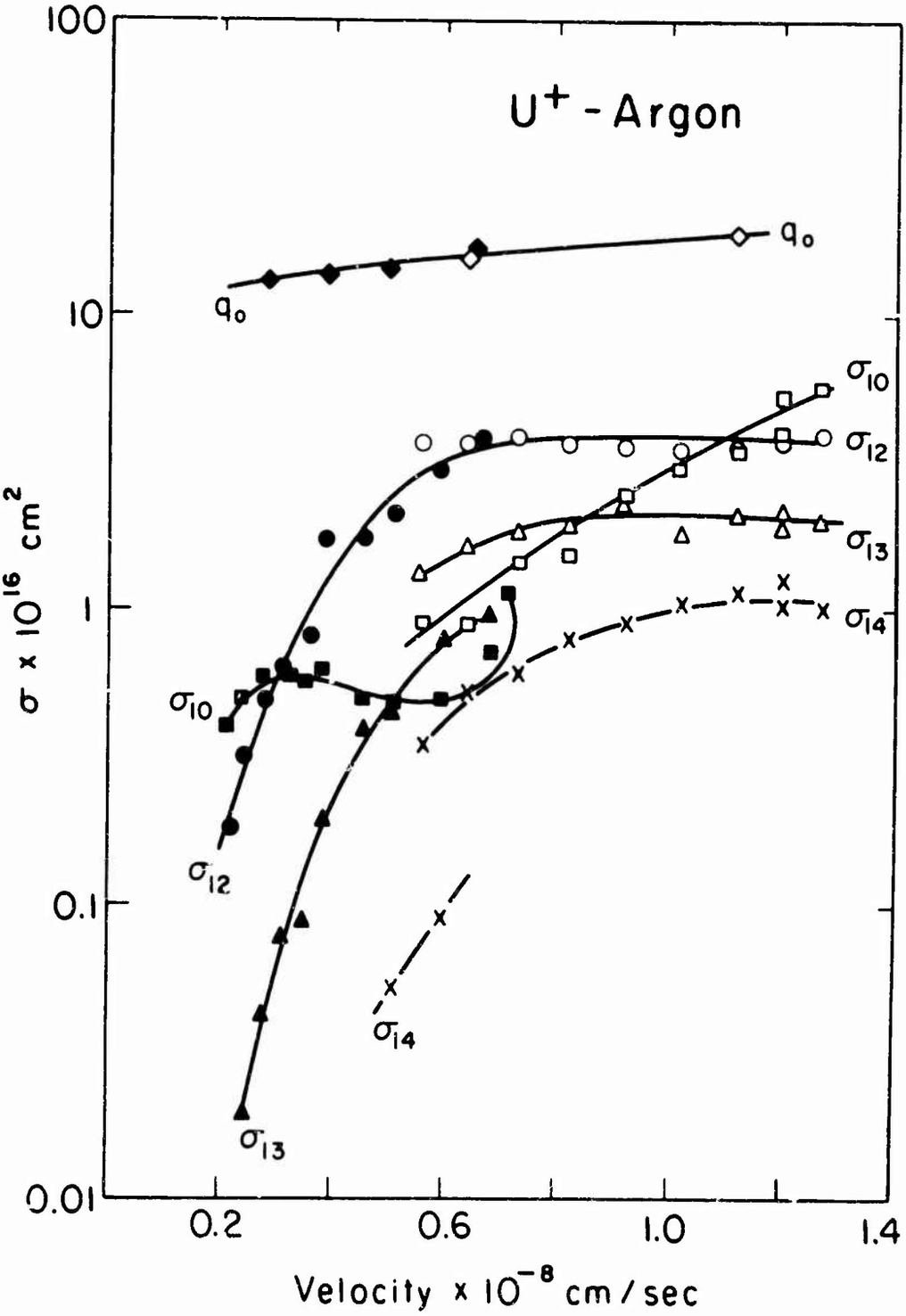

Note: Data taken earlier (Ref. 1) at the lower energies are indicated by solid data points and the most recent data by the open data points.

Figure 16. Electron Capture and Loss Cross Sections of U^+ in Ar

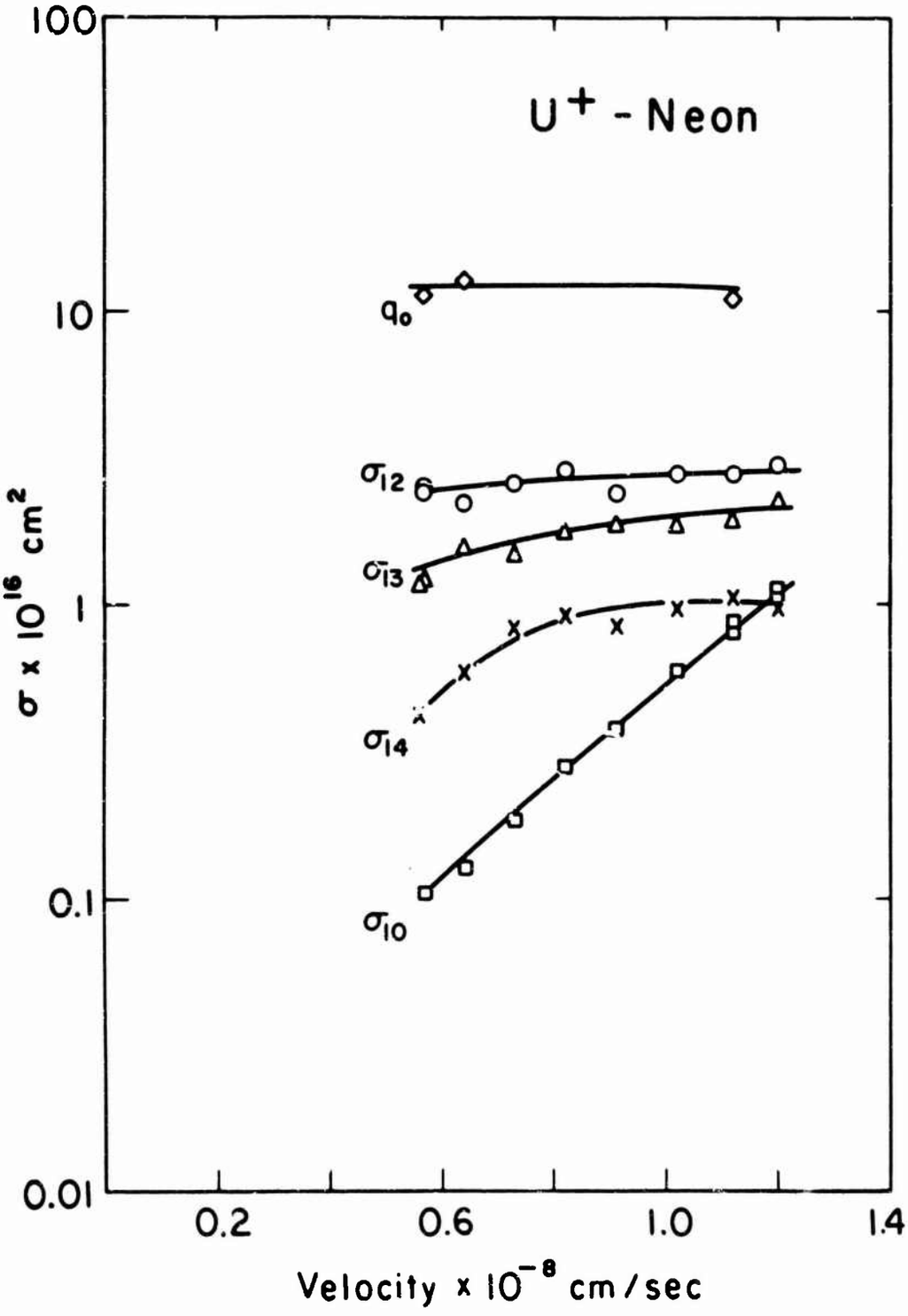

Figure 17. Electron Capture and Loss Cross Sections of U^+ in Ne

If this is indeed the correct interpretation, as the data suggest might be the case, then it would appear appropriate to scale up the older results to where they coincided at the point of energy overlap with the newer results. We suggest that this procedure be followed in making applications of these cross sections, pending further clarification of the data.

SECTION III

ELECTRON-ION COLLISION EXPERIMENTS

1. Theory of the Experiments

Among the processes of interest for upper atmospheric effects of atomic weapons are those involving the collision of electrons with ions. These processes include dissociative recombination, excitation of radiation, electron-impact production of ions in metastable states, and dissociation of molecular ions. Since ions are chemically unstable, it is suggested that a crossed beam experiment be performed similar to those that have been successful in studying chemically unstable neutral species (such as atomic hydrogen), and for several years such experiments have been performed. Dolder, Harrison, and Thonemann (Ref. 7) first measured electron-impact ionization of Ne^+ ions, and their technique has been successfully extended to measurements on ionization of many other ions in a number of laboratories.

The use of crossed beam experiments to study excitation in electron-ion experiments has not been so successful. If radiation is to be detected, one must contend with the fact that the electron beam that is energetic enough to produce a given photon will also produce brehmsstrahlung at the anode and other unwanted radiation in the same wavelength range and the signal-to-noise problem becomes extremely difficult.

In studying excitation of He^+ ions, Dance, Harrison, and Smith (Ref. 8) chose to concentrate on excitation to the $2^2S_{1/2}$ state because an ion in this state, being metastable, can be allowed to leave the region of the exciting electron beam before it is detected, and the problem of noise produced by the energetic electron beam can be avoided.

Only with great difficulty was the excitation of Ba^+

resonance radiation studied by Bacon and Hooper (Ref. 9). To avoid the electron-generated radiation noise problem, they used interference filters with a very narrow radiation bandwidth. While this approach has been demonstrated to be usable, it is unfortunately limited to the regions of the spectrum for which such interference filters can be made. In general, therefore, the approach holds little promise for experiments in the ultraviolet (which is the most interesting spectral region for ion excitation applications), where all known radiation detectors of appreciable sensitivity are notoriously broad-band.

Clearly, if excitation producing ultraviolet radiation is to be studied, an entirely different experimental approach is required, one which by some other means excludes the radiation noise produced by an energetic electron beam. Obviously one way to exclude this noise is not to use energetic electrons, but to get the relative velocity corresponding to the electron energy in the center of mass coordinates needed to produce a desired excitation by giving the energy in the laboratory coordinates to the ions rather than to the electrons.

The ion energies required to provide the requisite relative velocity if a stationary electron were to be hit are given by

$$E_{min} = (M/m)E_o \qquad (7)$$

where E_o is the threshold energy for the excitation, M is the mass of the ion and m is the electron mass. For the case of exciting He^+ to radiate its Lyman alpha radiation (304Å, 40.8 eV), where $M/m = 7350$, the minimum laboratory energy is 299 keV. For a number of strong excitation lines of ions, although the masses and the wavelengths vary considerably, the laboratory energies required work out to be of the same general magnitude. Such energies are very conveniently provided by the Van de Graaff

accelerator, and it is suggested that one can use the Van de Graaff and shoot ions through a cloud of electrons and observe the radiation emitted without the troublesome electron noise.

a. Effective Electron Energy Considerations

In any practical application of this approach, account must be taken of the fact that the electrons are not stationary but have a Maxwellian distribution in the laboratory frame. It is straightforward to show (Ref. 10) that in the ion's frame of reference the distribution of electron energies is given by

$$P(E)dF = \sqrt{\frac{2}{\pi mkT}} \; \frac{e^{-\frac{mV^2}{kT}}}{V} \; \sinh\left(\frac{V}{kT}\sqrt{2mE}\right)dE \qquad (8)$$

where V is the velocity of the ion in the laboratory coordinates, m is the electron mass, and T is the temperature of the electron gas in the laboratory frame.

The moments of this distribution function are

$$\bar{E} = \tfrac{1}{2} m(V^2 + 3kT/m)$$

$$\overline{E^2} = \tfrac{1}{4} m^2[V^4 + 10V^2(kT/m) + 15(kT/m)^2] \qquad (9)$$

The root mean square deviation from the mean energy $\bar{E}$ is

$$\Delta E = \sqrt{\overline{E^2} - (\bar{E})^2} = \tfrac{1}{2} m \sqrt{4V^2(kT/m) + 6(kT/m)^2} \qquad (10)$$

Evaluation for the case of He^+ ions traveling at an energy of 300 keV through an electron cloud at a temperature of 3000°K indicates that $\bar{E}$ = 41 eV and ΔE = 4.5 eV. Particularly to be noted is that the mean square deviation from the mean energy (the effective half-width of the electron energy distribution) is 4.5 eV in the ion frame of reference as opposed to the approximately

0.25 eV in the laboratory frame. The approach of using fast ions enormously broadens the effective electron energy spread.

Of interest in excitation studies is the question of the expected signal dependence at ion velocities below that at which an electron at rest in the laboratory has enough energy in the center of mass system to excite the ion. In order to estimate this signal dependence, we can take advantage of the fact that ion excitation processes are believed on theoretical grounds to have a finite cross section at threshold and can approximate such a cross section by a step function. Evaluating the excitation probability per ion per unit time, R, with such a cross section yields

$$R = n\sqrt{\frac{2kT}{\pi m}}\left(e^{-\frac{m}{2kT}(v_o-V)^2} + e^{-\frac{m}{2kT}(v_o+V)^2} \right) + n\sqrt{\frac{m}{2\pi kT}} \cdot \frac{1}{V} \int_{v_o-V}^{v_o+V} e^{-\frac{m}{2kT}u^2}(u^2 + V^2)du \qquad (11)$$

where n is the electron number density, and v_o is the threshold electron velocity in the center of mass coordinates. In cases such as helium ion excitation, where $v_o = 3.8 \times 10^8$ cm/sec and for T = 3000°K, so that $mv_o^2/2kT >> 1$, Eq. (11) simplifies to

$$R = 2n\sqrt{\frac{m}{2\pi kT}}\; v_o\, e^{-\frac{mv_o^2}{2kT}}\left[1 + \frac{2}{3}\left(\frac{mv_o}{2kT}\right)^2 V^2\right] \qquad (12)$$

At values of V such that $mV^2/2kT \gtrsim 1$ (i.e., ion energies $\gtrsim$ 2 kev), the unity in the term in parentheses can be neglected leaving $R \propto V^2$. Since the signal is related to R, the length in the experiment and the ion velocity by S = RL/V, the signal strength

at low V is given by

$$S = \frac{4n}{3}\sqrt{\frac{m}{2\pi kT}}\; v_o^2 e^{-\frac{mv_o^2}{2kT}} \left(\frac{mv_o^2}{2kT}\right)^2 \cdot L \cdot V \qquad (13)$$

It is seen, therefore that a finite threshold will identify itself by having a linear dependence of signal with ion velocity at low energies. In a similar way, analysis of the dependence of the signal on V can serve to map out the essential features of an ion excitation cross section.

b. Production of Electron Clouds

To produce electron clouds, the first arrangement considered in the present experiments was the space charge limitation inside a thermionically emitting hollow tube. Such tubes are attractive because their construction is standard practice in this laboratory for use as thermal dissociation sources of atomic beams.

Of principal concern to the design of the present experiments are (1) the number density of electrons under space charge conditions inside such a tube, and (2) the spatial distribution of electrostatic potential. These questions can be answered by straightforward calculation. We take the case of an infinitely long cylindrical tube of radius a and set up Poisson's equation in cylindrical coordinates

$$\frac{1}{r}\frac{d}{dr}\left(r\frac{d\phi}{dr}\right) = 4\pi e n(r) \qquad (14)$$

Under conditions of equilibrium, n(r) is given by the Boltzmann relation

$$n(r) = n_w e^{e\phi/kT} \qquad (15)$$

where n_w is the number density of electrons at the walls of the tube. By substituting Eq. (15) into (14) and integrating subject to the boundary conditions that at r = a, $\phi(a) = 0$, we have

$$\frac{\sqrt{1 + \frac{C}{2} r^2 e^u} - 1}{\sqrt{1 + \frac{C}{2} r^2 e^u} + 1} = \frac{\sqrt{1 + \frac{C}{2} a^2} - 1}{\sqrt{1 + \frac{C}{2} a^2} + 1} \cdot \frac{r^2}{a^2} \tag{16}$$

where $C = \frac{4\pi n_w e^2}{kT}$ and $u(r) = \frac{e\phi}{kT}$.

By rearranging Eq. (16), we can write

$$u(r) = \log_e \left\{ \frac{2}{cr^2} \left[\left(\frac{1 + p \frac{r^2}{a^2}}{1 - p \frac{r^2}{a^2}} \right)^2 - 1 \right] \right\} \tag{17}$$

where $p = \frac{\sqrt{1 + \frac{C}{2} a^2} - 1}{\sqrt{1 + \frac{C}{2} a^2} + 1}$.

In order to know the value of C, it is necessary to determine n_w, and this can be done by equating the flow of electrons away from and toward the thermionically emitting walls of the tube. By the Richardson-Dushman law, the current density away from the walls is given by

$$J = AT^2 e^{-W/kT}$$

where A = 60.2 amperes/cm^2-deg^2 for tungsten and W is the work function. Since the electron gas is in equilibrium, the current density of

electrons effusing to the walls is given by

$$J = \tfrac{1}{4} n_w e(8kT/\pi m)^{1/2}$$

from the kinetic theory of gases. Equating these two expressions, we have

$$n_w = \frac{A}{e}\sqrt{\frac{2\pi m}{k}}\ T^{3/2} e^{-W/kT} \qquad (18)$$

For tungsten, with a work function of 4.5 ev, working at a temperature of 3000°K, n_w is approximately 6×10^{12} cm^{-3}.

It is recognized that the constant C, defined in Eq. (16) is just the inverse of the square of the Debye length in the immediate vicinity of the wall. For tungsten at 3000°K, the value of C is approximately 4.2×10^{7} cm^{-2} and the Debye length is approximately 1.6×10^{-4} cm, i.e., very much less than the tube radius. For a tube of radius 2 mm (4 mm i.d.), $Ca^2/2$ is approximately 8.4×10^{5}, which is very much greater than unity. Under these circumstances the quantity p, defined in Eq. (17), can be replaced by unity and that expression can be simplified to

$$u(r) = \frac{e(r)}{kT} = \log_e\left[\frac{8}{Ca^2\left(1 - \frac{r^2}{a^2}\right)^2}\right] \qquad (19)$$

(Equation (19) fails at r = a because of the approximation p = 1. As r → a, the full expression of Eq. (17) must be evaluated in a limiting procedure.)

For r = 0, with $Ca^2 = 1.7 \times 10^{6}$, the potential along the axis has the value of approximately -3.2 eV. Evaluation of Eq. (19) at r = a/2 gives $\phi \cong -3.1$ eV, which indicates the very important point that (under space charge conditions) the potential along the radius of the tube is very nearly flat. The drop in potential occurs at the walls where the fields become as large as 750 volts/cm.

From n_w (6×10^{12} cm^{-3}) and the potential on the axis (-3.2 eV), it is found immediately from Eq. (15) that the number density of electrons along the axis of the tube is approximately 2.5×10^7 electrons/cm^3.

Referring again to the case of He^+ ions at a speed $V = 3.8 \times 10^8$ cm/sec traversing a space charge cloud of this type, the electron density as seen by the ion is the product of $nV = 1 \times 10^{16}$ electrons/cm^2-sec, about 0.6 mA/cm^2. If the ion traverses a distance of L cm over which signals can be detected, the probability of an event per ion is given by $Q \cdot nV \cdot (L/V) = nQL$ where Q is the cross section averaged over the electron energy distribution given in Eq. (8). Taking $Q = 10^{-18}$ cm^2 and L = 5 cm, the expectation of an excitation per ion is $2.5 \times 10^7 \times 10^{-18} \times 5 = 1.3 \times 10^{-10}$. By using an ion current of 10^{14} ions per second (approximately 10^{-5} amperes), approximately 10^4 photons per second would be produced.

c. Noise Considerations

In considering a photon detection experiment, noise that could mask the desired signals would in general be photons from extraneous sources. The first source of photons in the experiment conceived and described above is the thermal radiation from the 3000°K furnace. To avoid this source of noise, it is necessary to limit consideration of the approach only to processes where the photon wavelength is short compared to the photons from a black body source at 3000°K, and in general this means excitation processes with photon wavelengths in the vacuum ultraviolet (less than about 1000 Å). He^+ excitation with a 304Å photon nicely satisfies this need.

The major source of noise anticipated for the He^+ excitation experiment was that expected to come from charge transfer of the He^+ ions with residual gases in the vacuum chamber where the

neutral He ended up in the 2^1P state, radiation from which produces a photon at 584Å. Since the cross section for charge transfer of He^+ to produce helium resonance radiation has not been measured, it was impossible to know how serious this source of noise would be. In the anticipation that it would be a serious source of noise, considerable attention was given to the development of detectors and thin-film filters that would strongly suppress 584Å radiation while transmitting 304Å radiation reasonably well.

Beyond this, it was necessary to try the experiment to discover whether other sources of noise would prove serious. Such a preliminary trial was made early in the contract period. The results did not show any sources of noise that would be catastrophically large. Thereupon, the development of thin-film filters was undertaken, and the experiment was repeated, primarily to further assess noise problems on a more sensitive scale, although with the hope that some meaningful signals would be seen at the same time. The sections below discuss the experimental work and results obtained to date.

2. Experimental Considerations

a. Ion Source

The ion source used in these experiments is that shown in Figure 1. As noted in Section II-2 of this report, the ion source produced a resolved current after acceleration of approximately 1 micrcampere. The beam spot appeared to be about 5 mm in diameter after acceleration, and beam purification deflection, and only about 2 to 3 x 10^{-8} ampere could be injected through the aperture to the furnace end and collected beyond it. This current was substantially lower than what was desired for the experiment but was deemed sufficient to further examine the noise in the experiment and also possibly to detect signals using long counting times.

b. Furnace (Electron Cloud Target)

The electron cloud target is shown in Figure 18. The furnace was made of rolled 0.001 inch tungsten foil and operated at a power level of 800 watts in producing 3000°K temperatures. The tungsten tube was held by molybdenum tubes at both ends and was 29 mm long (between molybdenum tubes) and 4 mm in diameter. The molybdenum tubes were mounted into two water-cooled copper blocks and a water-cooled radiation shield surrounded the furnace. The tungsten tube had a slit of dimensions 0.8 mm x 20 mm running along its length and photons emerged from this slit to the detector, which was mounted above the furnace. The temperature of the furnace was measured by using an optical pyrometer that viewed into the gap between the last layer of foil and the main tube body. Under these conditions, the pyrometer read the temperature directly with no corrections being needed for emissivity of the tungsten.

The furnace was heated by dc current. It was necessary to use caution in running the current-carrying leads to the furnace in order to prevent the magnetic fields from these leads from affecting the electron orbits in the electron multiplier used to detect the photons. By running the two wires side by side except immediately at the furnace it was determined that a change of polarity (reversal of the magnetic fields) did not apparently affect the operation of the electron-multiplier-detected photon signals.

The current through the furnace was slightly less than 200 amperes, implying that a 4-volt drop occurred along the length of the furnace. This drop unquestionably affects the distribution of the electrons inside the furnace, but this problem has not been analyzed in detail.

Figure 18 also shows above the furnace a holder in which three thin-film filters could be placed. This holder could slide, thereby

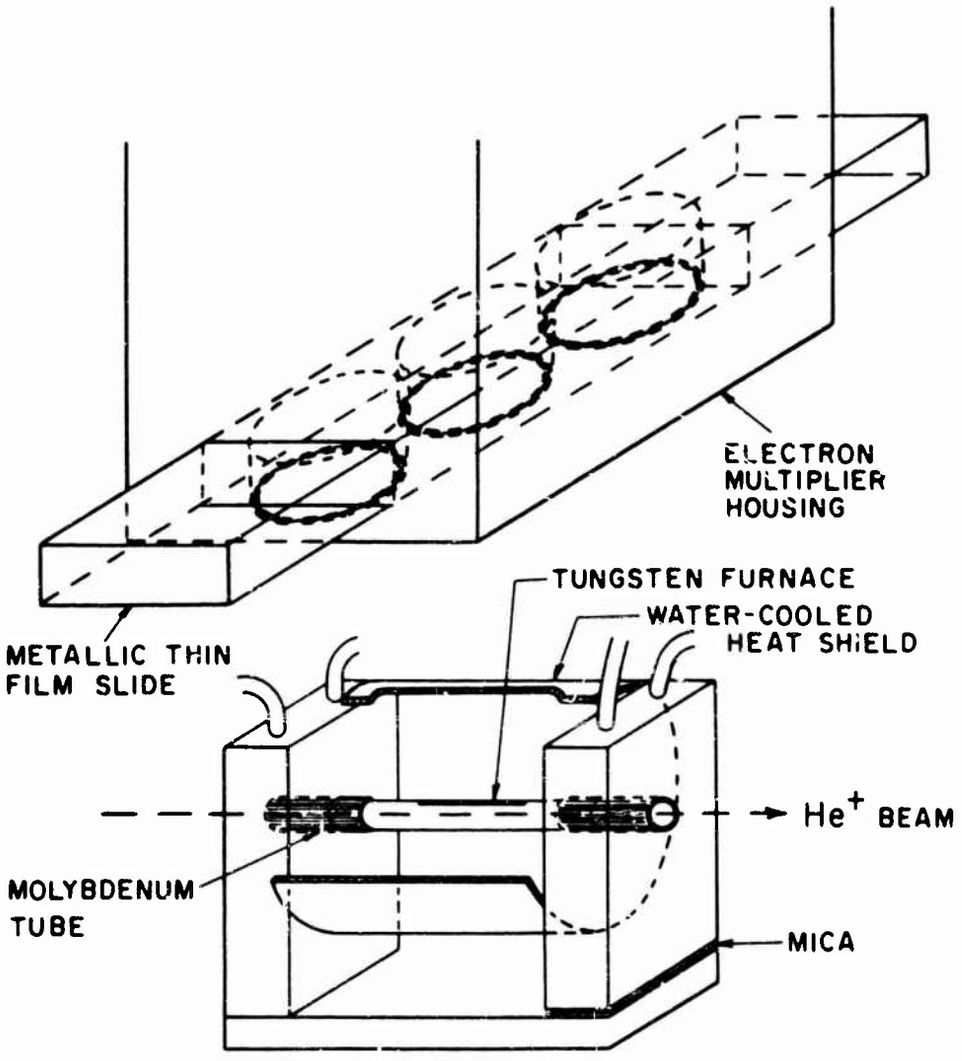

EXPERIMENTAL ARRANGEMENT FOR ELECTRON IMPACT EXCITATION OF IONS

Note: The electron space charge cloud is inside the tungsten furnace and light from the interaction proceeds upward, through thin-film filters to a radiation detector (not shown).

Figure 18. Experimental arrangement for Electron Impact Excitation of Ions

allowing different filters to be used during the course of an experiment. Located above the filter holder was the radiation detector.

c. Radiation Detectors and Filters

The first radiation detector planned for use was an ordinary open multiplier using Cu-Be surfaces (including the first dynode). Since the work function of Cu-Be is only about 4.2 eV it would respond to the black body radiation from the furnace and the electron multiplier had to be filtered against this thermal radiation. The principal background arising from the ion beam was expected to be the 584Å resonance radiation produced in charge transfer with the residual background gases and it was thought necessary to filter very strongly against this radiation.

The most promising approach to filter against these radiations while still passing the desired 304Å He^+ Lyman alpha appeared to be the use of a combination of carbon and aluminum thin-film filters (Ref. 11). The thin carbon filters are particularly suitable for transmitting the 304Å radiation while at the same time absorbing the 584Å resonance radiation. When the aluminum film is thicker than 800Å in thickness, it is completely opaque from the visible range down to 837Å at which point it starts transmitting. Consequently the aluminum film was used to correct for the fact that the carbon films transmit at wavelengths greater than 900Å.

(1) Preparation of Films

The unbacked aluminum thin films were prepared as follows. At a pressure of 10^{-6} torr, a layer of 1000Å thick sodium chloride, used as the parting agent, was evaporated from a tantalum dimple onto the glass microscope slides that were carefully cleaned and rinsed in order to avoid pinholes that are usually developed in

the thin films because of dust and grease on the substrate. This was immediately followed by evaporating aluminum, using electron beam evaporation source. After removal from the vacuum the aluminum film was floated off the slide onto a distilled water surface that was mechanically raised. The slide was set at an angle somewhere between 30° to 45° to the water surface. Finally the aluminum film was picked up on a 100 line/inch (75 percent optical transmittance) gold screen supported on circular stainless steel frame with a 5/8 inch hole.

Carbon films of 5^{+3}_{-2} μgm cm^{-2}, corresponding to thickness of 250^{+150}_{-100} Å, were procured commercially.*

Film thickness measurements were made both during evaporation and afterwards. In the vacuum chamber, measurements were made with a deposite thickness monitor,** which operates on the principle that the natural frequency of a quartz crystal will change if its mass is increased by depositing dielectric or metal films on it. The thickness of several samples as determined above was checked by using an angstrometer which operated on the principle of a Tolansky interferometer. Satisfactory agreement between thickness measurements by using the two different methods of measurements was found.

(2) Testing Transmission of Thin Films - Monochromator

In order to measure the transmittance of carbon, aluminum, and Zapon*** thin films, a grazing incidence vacuum ultraviolet monochromator was built, which scans the spectral region from 100Å to 2000Å. The entrance slit and grating were fixed, while the exit slit together with the electron multiplier detector was mounted on the end of a level arm, which can be rotated around the center of the Rowland circle.

---

* Yissum Research Development Company, Jerusalem, Isreal

** Sloan DTM-2A

*** Cellulose Acetate

In a Paschen-Runge mounting, the entrance slit, grating, and the diffracted spectrum lie on the Rowland circle that has as its diameter the radius of the curvature of the grating. The grating equation is given by

$$m\lambda = a(\sin \alpha + \sin \beta) \tag{20}$$

where

m = the order of the spectrum
a = the grating space
α = the angle of incidence
β = the angle of diffraction

and the signs of α and β are opposite when they lie on different sides of the grating normal.

On the present case, a 40-cm concave grating (20 x 20 mm^2) with 600 lines/mm was used. The angle of incidence was 80.3 degrees. The dispersion in the first order was 17Å/mm. The two slit widths were 0.2 mm.

The light source used for the monochromator was an uncooled radio frequency discharge source made by leaking helium gas into a 7 mm quartz tube. The tube had a 0.25 mm hole in the end that pointed toward the entrance slit of the monochromator. The helium spectrum was dominated by the first resonance line of neutral helium at 584Å. The 304Å He II Lyman alpha line was down in intensity by about a factor of 5.

The entrance slit was placed on a flange that separated the chamber of light source and that of the monochromator. These two chambers were pumped out by separate mercury diffusion pumps, which permit vacuum of 1 x 10^{-5} (with light source turned on) and 4 x 10^{-6} torr in the light source and monochromator chamber, respectively.

In testing, films were mounted in the vertical sliding

holder (See Figure 18), which was placed immediately behind the entrance slit. The output of the electron multiplier* operated at 3000 volts was fed into an electrometer** which, in turn, drove a pen recorder. With exit slit set at the specific wavelength of radiation signals were measured with and without films in the light beam. After correcting for the background that is caused by the scattering of the light beam, the ratio of signal obtained with film to signal obtained without film determined the transmittance of the film tested. Both carbon and aluminum thin films were examined at wavelengths of 304Å and 584Å. A typical result is shown in Table I.

TABLE I

TRANSMITTANCE (IN PERCENT) OF CARBON AND ALUMINUM FILMS

FILM	RADIATION 304Å	584Å
C (480Å thick)	11	0.03
Al (600Å thick)	55	18
one C (500Å thick) and two Al (600Å thick)	3.85	1/460

(3) Geiger-Mueller (GM) Counter Detector

In the course of the work on thin-film filters described above, it was found that pinholes frequently developed in the films, evidently after they were constructed. The effect of such pinholes

*Dumont SPM 301-03-303

**Keithley Model 600A

could be minimized by using two or more thin film filters in series rather than a single film of greater thickness. However, it was felt desirable to construct other films with greater mechanical integrity and the work of Ederer and Tomboulian (Ref. 12) suggested that Zapon be considered. Although the absorption spectrum of Zapon films over the entire spectral range of importance in the present experiments was not known, it was known that it would transmit at 304Å, and the option remained of supplementing the Zapon films with carbon and aluminum filters to correct for any other transmission problems.

The fact that the transmission of Zapon at 304Å with films of reasonable thickness is less than 10 percent recommended that a more sensitive detector of the transmitted photons than an open multiplier be used. The most obvious alternative to the multiplier (whose dynode surfaces have a photoelectric efficiency of only about 6.5 percent at 304Å) was a Geiger-Mueller counter in which the gas to be photoionized would be helium. By properly choosing the geometry of a GM counter and the helium gas pressure, one should be able to construct a detector with an efficiency approaching unity. Further, by variation of geometry, it should be possible to have the counter work well at a gas pressure that could be contained by a suitably braced Zapon film. It was accordingly decided to develop such a GM counter for use in these experiments.

The counter was made of stainless steel, with a collector wire mounted coaxially. The counter was 5.1 cm long and 1.9 cm inside diameter. The central wire was tungsten and had a diameter of 0.002 inch. The window was located in the side wall of the counter and was sealed to the side using an O-ring arrangement.

In making Zapon films, solution of 0.1 gm cellulose acetate in 13 ml of methyl acetate was prepared. One drop of this solution picked up by a dropper with 1.5 mm mouth was dipped onto distilled

water that was cooled to 0°C. Zapon was then lifted up with a wire loop and placed over a stainless steel window frame on which a fine nickel screen (500 lines/in. with 52 percent transmittance) was previously cemented. To minimize the possibility of leaks, two layers of Zapon were placed on the frame.

By using the monochromator, it was found that the window prepared by this way had about 7 percent transmittance for 304Å. The transmittance at 584Å was two to three orders of magnitude less.

The GM counter was operated in the self-quenched mode with a dead time of approximately 30 usec. The counting gas was a mixture of helium and isobutane (96 percent He and 4 percent C_4H_{10}). The negative pulses were brought out from the central wire by a coaxial cable and were amplified and displayed on an oscilloscope whose gate was then connected to a scaler. Typical operating conditions of the counter were that the pressure of the counting gas was 50 torr and the voltage across the counter was 715 volts.

Since the Zapon window can withstand a pressure difference of only about 150 torr, it was necessary to use a special gas filling system allowing the counter to be evacuated simultaneously with the main chamber in which the excitation experiment was performed.

3. Measurements

In the experimental arrangement ions from the ion source were mass filtered by the RF quadrupole and accelerated by the Van de Graaff accelerator. The He^+ ions traveling at sufficient speed to cause the excitation were shot through the electron cloud produced in the cylindrical tungsten furnace at 3000°K. After leaving the collision region, the ion beam was collected in a deep Faraday cup. Photons produced between the electron-He^+ collisions were detected by either the electron multiplier or the Geiger-Mueller counter, preceded by one carbon (480Å thick) and

two aluminum (600Å thick) thin-film filters. Two aluminum filters were used in series to minimize transmission of light through pinholes, which were very difficult to fully exclude from the aluminum films. The detector was 10 cm above the tungsten tube.

The output pulses of the electron multiplier were preamplified and then fed into the oscilloscope, which in turn drove a scaler. The electronics used for the GM counter was already mentioned in Section III-2, C(1).

Signal measurements were made in the following manner:

(a) At a particular ion energy, the He^+ ions were shot through the electron cloud, and the photon count recorded. This signal included the (1) electron-ion collision signal, (2) noise associated with the hot furnace through black body radiation and any noise generated by the electrons in the furnace and (3) any noise associated with the ion beam but not involving the electron-ion interaction, and (4) any electronic circuitry noise, cosmic ray background, etc.;

(b) Next, with the furnace cooled, the photon count reflected only noise from sources (3) and (4) above;

(c) With the ion beam shut off and the furnace turned on, the signal indicated noise sources (2) and (4) above;

(d) With both the ion beam and the furnace turned off, noise source (4) was displayed.

By algebraic combination of the four signals the four sources of signals were separately assessed. The 304Å signal should be given by a - b - c + d.

Typical early data taken using ion energies from 500 to 900 keV by using the GM detector preceded by two Al films and one C film are presented in Table II.

Clearly one should completely ignore the apparent 304Å signals in this table in view of the enormous scatter of values (including negative values) compared to the statistical uncertainties. Additionally, reasonable estimates of the expected 304Å signals

TABLE II

SIGNAL MEASUREMENTS FOR EXCITATION OF He^+ IONS

Item	Ion Energy (keV)	Ion Current 10^{-8} amp	Ion Beam On		Ion Beam Off		304Å Apparent Signal Counts per 100 seconds	Signal Counts per 100 seconds at 10^{-8} amp
			Furnace on Counts per 100 seconds (a)	Furnace off Counts per 100 seconds (b)	Furnace on Counts per 100 seconds (c)	Furnace off Counts per 100 seconds (d)		
1	500	0.4	322	64	221	4	41 (±25)	103 (±60)
2	600	0.4	1036	631	305	12	112 (±45)	280 (±110)
3	600	0.4	1195	656	493	5	51 (±48)	122 (±120)
4	600	1.2	4279	3554	81	8	652 (±89)	543 (±74)
5	700	1.9	3557	4280	83	10	-796 (±89)	-418 (±47)
6	800	1.8	3970	3200	228	9	551 (±86)	306 (±53)
7	900	1.45	1239	1105	62	12	134 (±49)	92 (±34)
8	900	1.85	1257	1265	54	7	-130 (±50)	-90 (±27)
9	900	1.85	1555	1427	133	11	6 (±56)	3 (±30)

Indicated Uncertainties from Counting Statistics Only.

under the experimental conditions are much smaller than even the statistical uncertainty.

Table II does elucidate, however, some of the principal noise features in this experimental approach. First, the values found in column (c) indicate that some noise is being produced by the furnace alone. Second, the large values in column (b) indicate that there is substantial noise generated by the ion beam, irrespective of whether the furnace is on or off.

The large values in column (b) would be consistent with 584Å signals from charge transfer in the residual gas, and to test this, the residual gas pressure was varied in the vacuum chamber. It was found however that the counts were not noticeably dependent on the gas pressure, apparently indicating that the 584Å radiation problem has been beaten through the use of Carbon films.

Insertion of a LiF window between the cold furnace and the detector completely stopped the signal, suggesting that the ion beam noise is radiation of wavelength less than 1050Å, the cut-off of lithium fluoride. The fact that carbon filters (which are opaque between about 600Å and the LiF cut-off) passed the radiation seems to indicate that the radiation was of wavelength less than 500Å.

Observing that the ion beam noise appeared to depend on the ion beam focusing conditions suggested that the photons might be produced when ions struck the walls of the furnace. A separate experiment was set up, in which a cold tungsten surface was bombarded by the He^+ beam and the impact point was viewed by the Geiger-Mueller tube detector preceded by carbon films. Ample counts were observed, indicating that photons are readily produced by ions striking the surfaces and studies of the attenuation of carbon films as a function of ion energy strongly suggest that the radiation extends from about 100Å to 300Å, with the intensity of the shorter wavelengths

increasing as the ion energy is increased from 100 keV to 600 keV. Further experiments in which attenuation characteristics are studied, using several films of different materials and thicknesses, should produce a more positive identification of this noise radiation spectrum.

4. Prognosis and Future Plans

It is too early to give a prognosis for the success of this experimental approach when applied to the excitation of He^+. Clearly the noise, which we currently hypothesize is generated when the ions strike surfaces, needs to be investigated somewhat further. If this is the correct interpretation, it can probably be corrected by a change of furnace geometry. It is a little worrisome that the 584Å problem was beaten a little too easily, and it is appropriate to examine briefly the process of charge transfer of He^+ with background gases producing He in the 2^1P state before a prognosis is pronounced.

It also is becoming clear that the He^+ excitation problem was perhaps not the wisest choice of problems on which to test the general approach of imparting energy to the ions in electron-ion collision studies because of the low cross section and the radiation detection problem. However, with increasing experience with the techniques in this general experimental approach more of its capabilities are becoming evident, and we remain optimistic that it will prove to be a fruitful way of obtaining certain types of data that are extremely difficult to obtain in any other known ways.

SECTION IV

EXCITATION OF 3914Å N_2^+ RADIATION IN COLLISIONS OF HEAVY IONS WITH N_2

1. Introduction

Collision-produced excitation of the (0,0) transition of the first negative bands of N_2^+ has received considerable attention over the past years because of the importance of this radiation in aurora, airglows (both natural and induced) and gas discharges. Most of the experiments have studied excitation of this radiation, which occurs at 3914Å, by electron impact on neutral N_2, (Ref. 13 through 20) detecting the radiation with photomultipliers that had been calibrated against standard lamps. The electron impact results were generally in good agreement as far as shape of the excitation function curve is concerned, but the absolute cross section curves have tended to cluster about two curves, one having values about twice those of the other. The later and presumably more reliable results (Ref. 16 through 20) cluster very well around the higher curve, which displays a maximum in the cross section of about 1.5×10^{-17} cm^2 at an electron energy of about 100 eV.

Some results are also available for proton impact excitation of this radiation (Ref. 14 and 21 through 24) with considerable disagreement again appearing in the absolute magnitudes of the cross section. Measurements for various other light ions, including N^+ and N_2^+ have also been reported, (Ref. 23 and 25) with energies extending up to 65 keV.

The purpose of the present experiments was to extend the range of data on ion impact excitation of this radiation by using both heavier ions and ion energies from 50 keV to 2 MeV.

The process under consideration is

$$A^{n+} + N_2 \rightarrow N_2^+(B^2\Sigma_u^+) + A^{m+} + (m - n + 1)e$$

followed by

$$N_2^+(B^2\Sigma_u^+,\ v' = 0) \rightarrow N_2^+(X^2\Sigma_g^+,\ v'' = 0) + h\nu$$

where A^{n+} is a heavy ion with a charge of +n.

Measurements were made with ion beams of Ba^+, Ba^{++}, Xe^+, N^+, O^+, and N_2^+ passing through nitrogen gas contained in a collision chamber. Photons were detected at 90° with respect to the ion beam direction by using a photomultiplier preceded by an interference filter. When N_2^+ beams were used, no distinction was made between simultaneous ionization and excitation of the target molecule and excitation of the incident ion in collision with the target neutral.

2. Experimental Arrangement and Procedures

The beam of ions was produced at the terminal of the Van de Graaff accelerator, mass-selected by an rf quadrupole mass filter located in the terminal and then accelerated. After acceleration, a 2° deflection of the ion beam was made by using a transverse electric field in order to purify the beam by removing primary ions that had changed charge and background gas ions formed through charge transfer or ionization along the length of the acceleration column, or a combination of both. Some 60 cm after the deflection purification, the beam was collimated and entered the collision chamber. Since the pressure in the vacuum between the purification deflection and the collision chamber was about 10^{-6} torr, from the known capture and loss cross sections (see Section II and References 1 and 2) it can be assured that alterations in the ion beam constituents, caused by collisions in the vacuum following purification, would be substantially less than 1 percent.

The essential parts of the present experiment are shown in

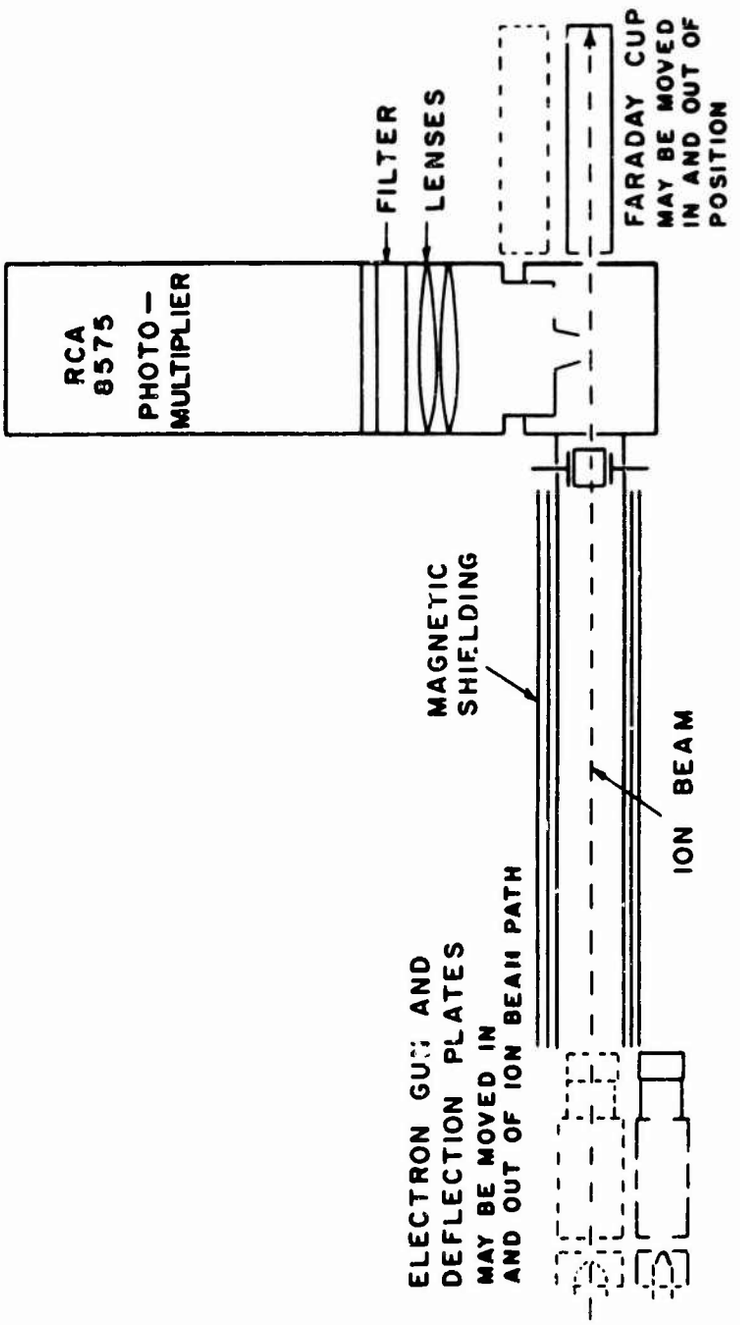

Note: The removable electron gun is used alternatively with the ion beam and a comparison of the signals observed yeilds the ratio of the cross sections for electron impact and ion impact excitation.

Figure 19. Experimental Arrangement for the Study of Excitation of 3914Å Light in Collisions of Ions with N_2

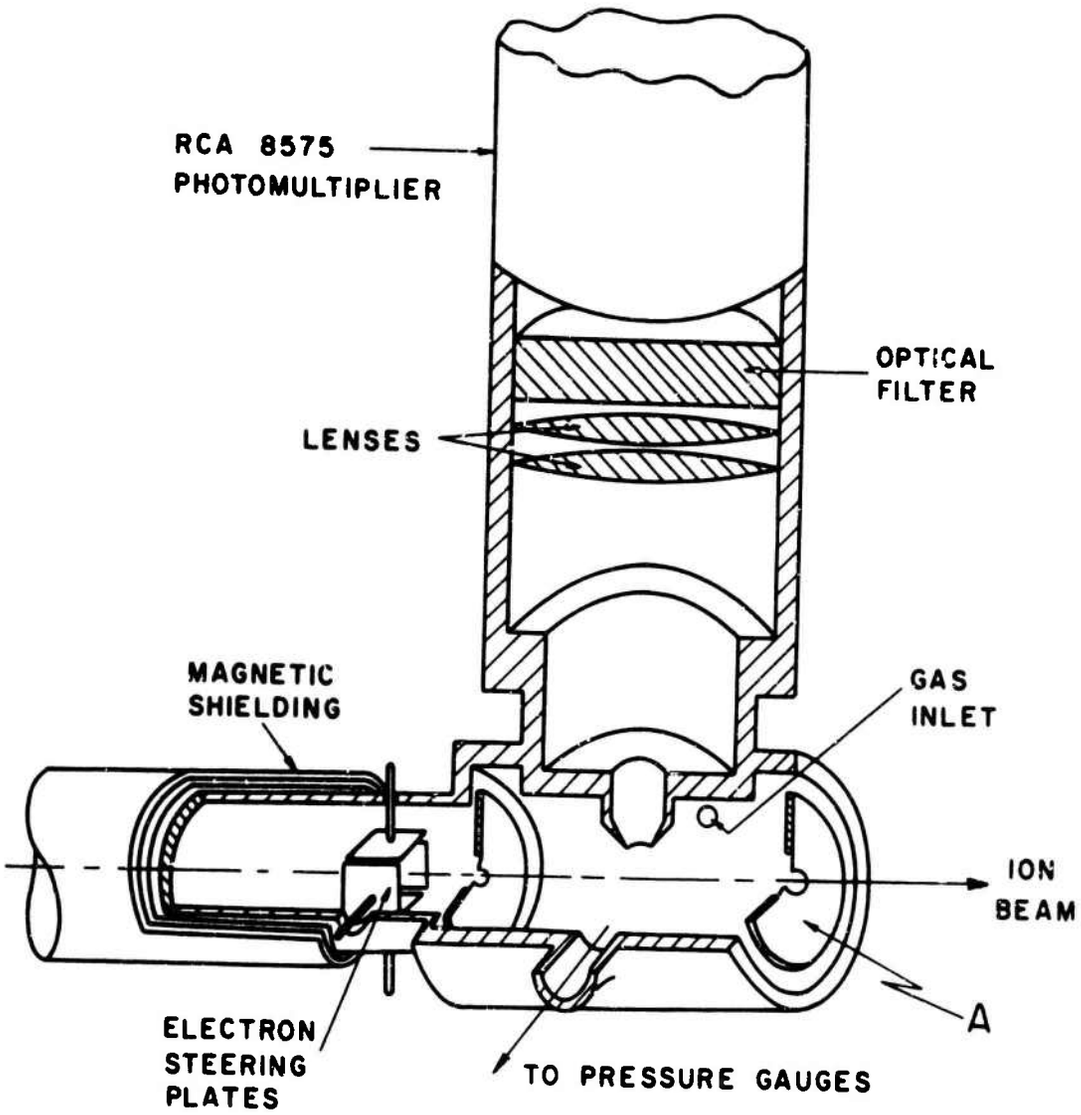

Figure 20. Details of the Collision Chamber and Optics in Studying Excitation of 3914Å Radiation

Figures 19 and 20. The ion beam proceeded from the left and entered the collision chamber, which had a diameter of 4.1 cm and a length of 5.5 cm. The beam entered the chamber through a circular aperture of 1 mm diameter and emerged through a horizontal slit of dimensions 2 mm x 5 mm. By using a moving detector of narrow aperture behind the exit slit, measurements of the scattering of the ions were made and assurance gained that all ions entering the chamber were indeed emerging from the collision chamber and entering the deep Faraday cup used to measure the ion currents.

Further assurance of correct ion current measurement was obtained by having the end walls of the collision chamber electrically insulated from the grounded main body of the collision chamber and by monitoring the current to the exit end plate concurrently with the Faraday cup current. With no gas in the collision chamber the end plate current was about 1 percent of the current measured to the Faraday cup. At the highest gas pressures (10^{-3} torr) used, approximately 10 percent of the ions were typically scattered in the gas cell sufficiently to strike the end plate, with a corresponding drop in current to the Faraday cup being always noted.

Photons produced in the collision chamber were detected through a circular aperture of 6 mm diameter, the plane of which was located 6 mm above the ion beam path. The light was collected by a lens system of focal length 7.5 cm, which was located at this distance above the ion beam. After passing through the lens system, the parallel light beam passed through a thin-film interference filter of 2 inches diameter having a maximum transmittance of 25 percent at 3914Å and a half-bandwidth of 25Å. The photons were ultimately detected by a photomultiplier tube* operated at 1800 volts.

---

*RCA 8575

As shown in Figure 19, the ion beam normally passed alongside an electron gun located approximately 30 cm from the entrance to the collision chamber. This electron gun could be moved into a position such that its electron beam could be used to excite the radiation. Magnetic shielding was placed around the region of travel of the electron beam and two sets of steering plates were used to trim the electron beam until measurements of the currents to the exit end plate of the collision chamber indicated that the electron beam was following the same path through the collision chamber as the ions had. Determination of the ion excitation cross sections was made by comparing the signals by using the ion beam and the electron beam alternatively, as discussed below.

The vacuum system used in the experimental region was a two-stage differentially pumped system, each stage being pumped by a liquid nitrogen baffled 6 inch oil diffusion pump. The first stage contained the deflection purifier of the ion beam and the electron gun, the collision chamber being located in the second chamber. The second chamber, which pumped back into the first chamber, had a pressure in the 10^{-6} torr range in normal operation of the experiment.

Pressure measurements were made using a differential capacitance manometer operating between the collision chamber and the vacuum of the second differentially pumped vacuum stage. The procedure in taking measurements was to fill a gas reservoir to a pressure slightly greater than one atmosphere and let gas from the reservoir enter the collision chamber through a needle valve. The reservoir was connected through a second needle valve to an external forepump, which slowly evacuated the reservoir. As the reservoir was evacuated the pressure in the chamber diminished also. The manometer signal, measuring the collision chamber pressure, was put on the X axis of an X-Y recorder while the Y axis recorded the photomultiplier output signal. In this way a plot of photon signal vs. pressure was obtained immediately.

The manometer calibration and linearity were again established as described in Section II-2. The pressure measurements are believed to be uncertain by no more than ±5 percent.

The curves of photomultiplier signal vs. chamber pressure were quite linear up to pressures of about 5×10^{-4} torr. The slope of the curves in this region dS_i/dp is related to the cross section $Q_i(E_i)$ of an incident ion at an energy E_i by

$$\frac{dS_i}{dp} = KQ_i(E_i)I_i \tag{21a}$$

where I_i is the ion current and K is a factor that includes experimental geometry, efficiency of photon detection, and the conversion factor between pressure and molecular number density. When the electron beam replaces the ion beam a similar expression describes the slope,

$$\frac{dS_e}{dp} = KQ_e(E_e)I_e \tag{21b}$$

where the subscript e refers to the electron and where K has the same value as in Eq. (21a). Dividing the two expressions, the ratio of the ion to the electron excitation cross sections is

$$\frac{Q_i(E_i)}{Q_e(E_e)} = \frac{(dS_i/dp) \times I_e}{(dS_e/dp) \times I_i} \tag{22}$$

and becomes determined from the experimental data. Since the cross sections $Q_e(E_e)$ are known (Ref. 16 through 20), the absolute value of $Q_i(E_i)$ is readily determined. The electron energy normally used was 300 eV where the cross section was taken to have the value 1.3×10^{-17} cm^2.

The values of the ratio given in Eq. (22) were determined to 10 percent or less. The possibility of extraneous radiation contributing to the signal was checked by replacing the N_2 in

the collision chamber by Ar, Ne, H_2, and O_2. When using primary ions other than N_2^+, the radiation signals did not exceed 2 percent of the signals obtained under the same conditions with N_2 in the collision chamber. When N_2^+ primary ions at energies in the 500 keV range against O_2 in the collision chamber the detected signals were approximately 5 percent of those with N_2 in the chamber, indicating the magnitude of excitation of the N_2^+ ion in collision with a neutral as compared to collisions in which a neutral N_2 molecule is both ionized and excited.

No measurements of the polarization of the radiation were made and therefore no corrections have been introduced for the possibility of the radiation having different angular distributions when produced by different incident charged particles.

3. Results

The results of the measurements are presented in Figures 21 through 26. The heavy ion excitation cross sections are of the same magnitude as the proton impact cross sections reported by Carleton and Lawrence (Ref. 21), Sheridan, Oldenberg, and Carleton (Ref. 14), and Philpot and Hughes (Ref. 22), and about an order of magnitude higher than electron impact excitation cross sections for comparable velocities.

Figure 26 contains the data of Sheridan and Clark (Ref. 23) as well as our own for excitation by N^+. Although the experimental energy ranges did not overlap, the two sets of results appear quite consistent.

The data of Figure 25 are replotted in Figure 27 and the results of Doering (Ref. 25) at energies below 10 keV are also included in this semi-log plot.

SECTION V

ADDITIONAL ACTIVITIES

In addition to the major efforts described in the preceding sections, some additional instrumental design activities have been carried out. The additional work that was initiated has been concerned with the improvement of the ion optics through the use of pairs of electrostatic quadrupole lenses. The beam cross section is altered in the deflection purification (this process introducing astigmatism) and an attempt to preshape the beam in by purposely introducing compensating astigmatism.

This activity has been carried out by Dr. Peter Teubner, using a system separate from the Van de Graaff accelerator. No results of significance have been obtained as yet.

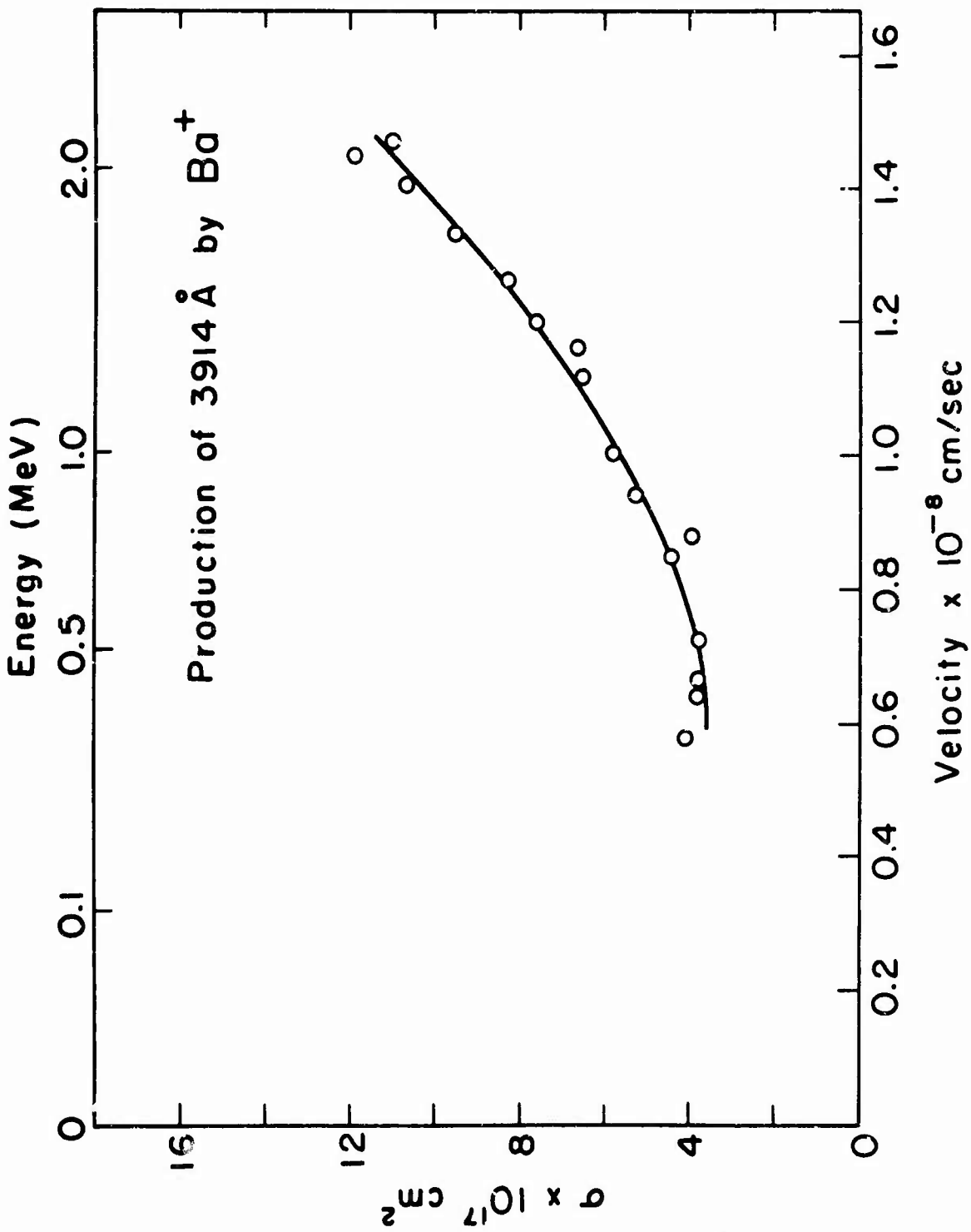

Figure 21. Cross Section for the Production of 3914Å Radiation in Collisions of Ba^+ in N_2

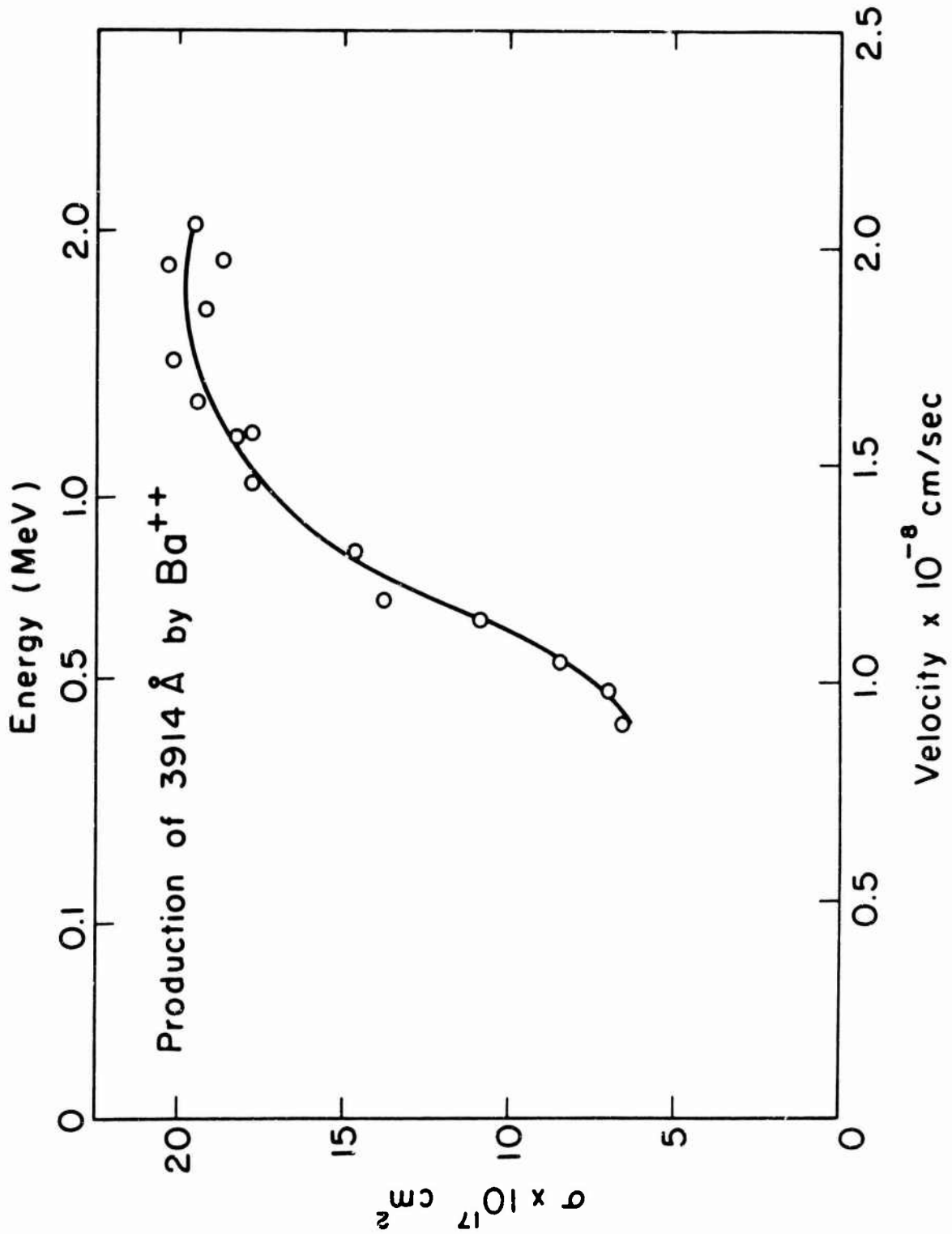

Figure 22. Cross Section for the Production of 3914Å Radiation in Collisions of Ba^{++} in N_2

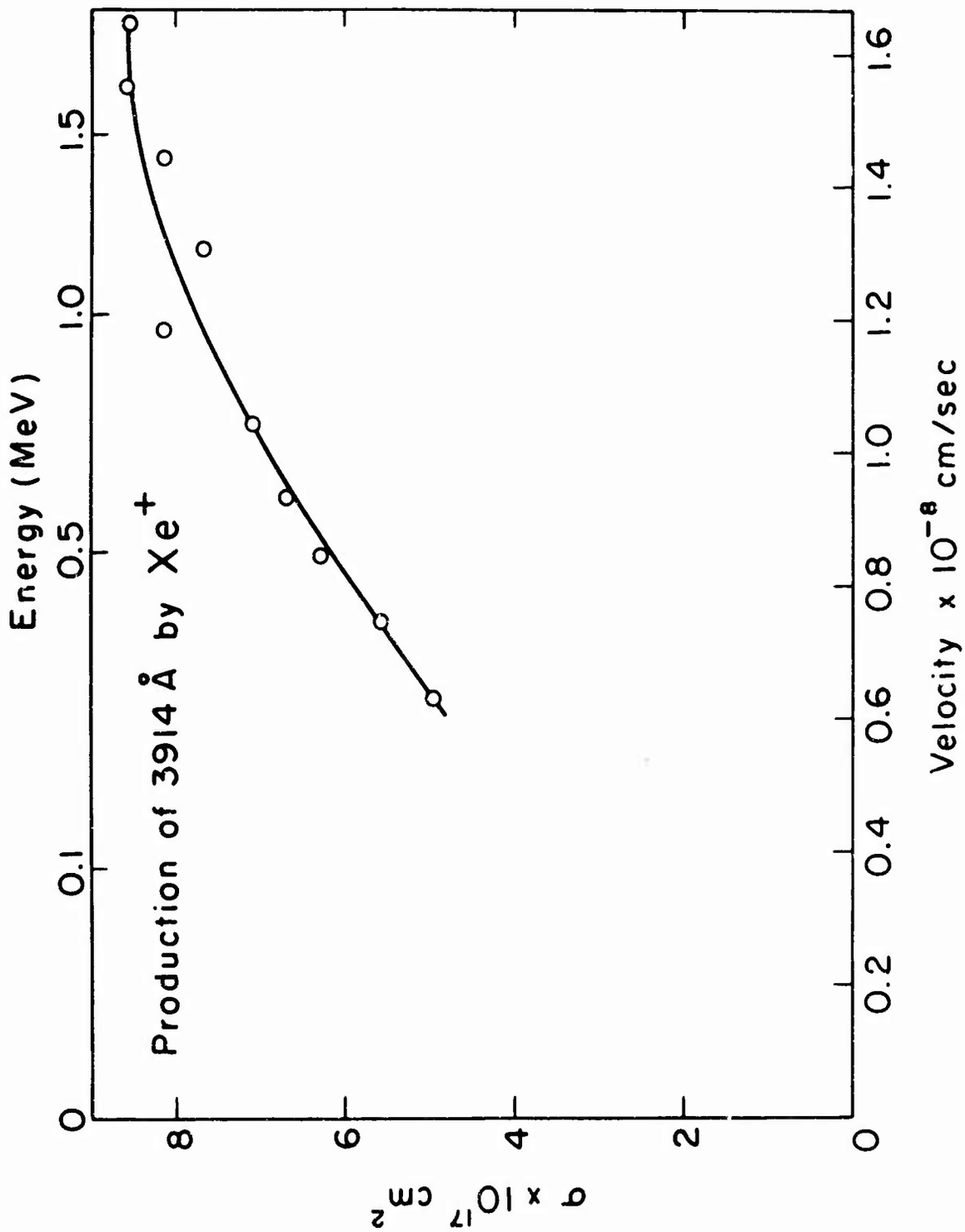

Figure 23. Cross Section for the Production of 3914Å Radiation in Collisions of Xe^+ in N_2

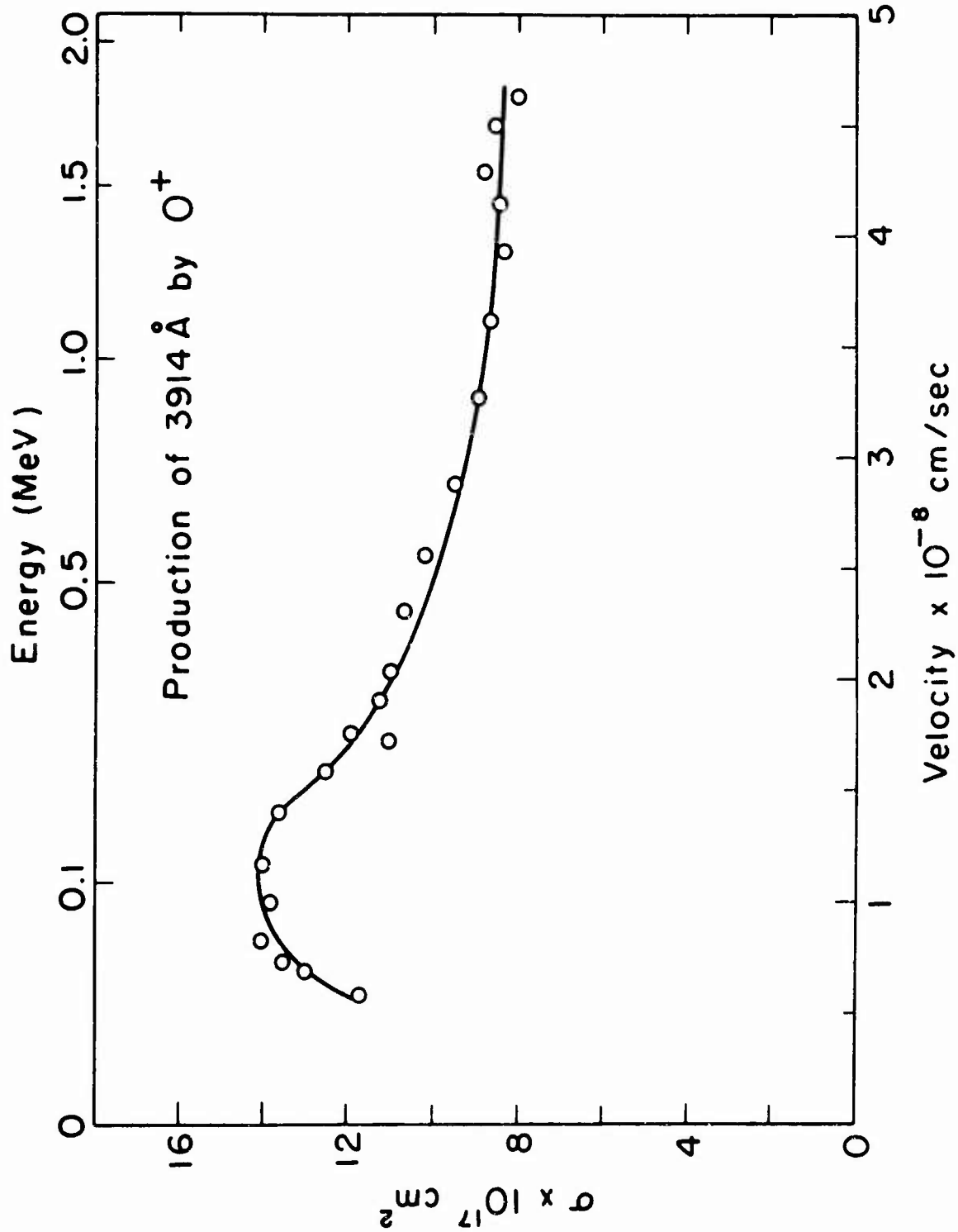

Figure 24. Cross Section for the Production of 3914Å Radiation in Collisions of O^+ in N_2

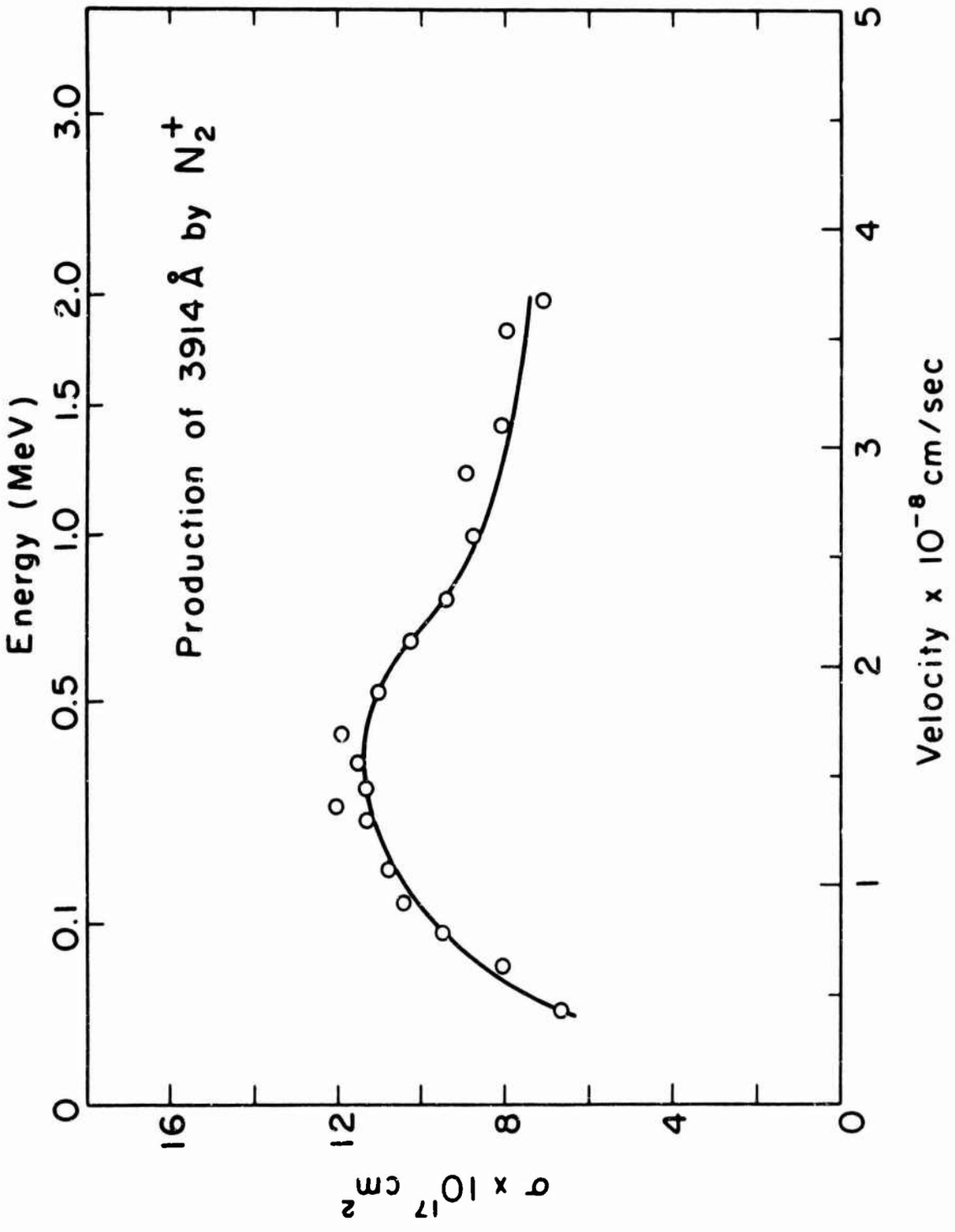

Figure 25. Cross Section for the Production of 3914Å Radiation in Collisions of N_2^+ in N_2

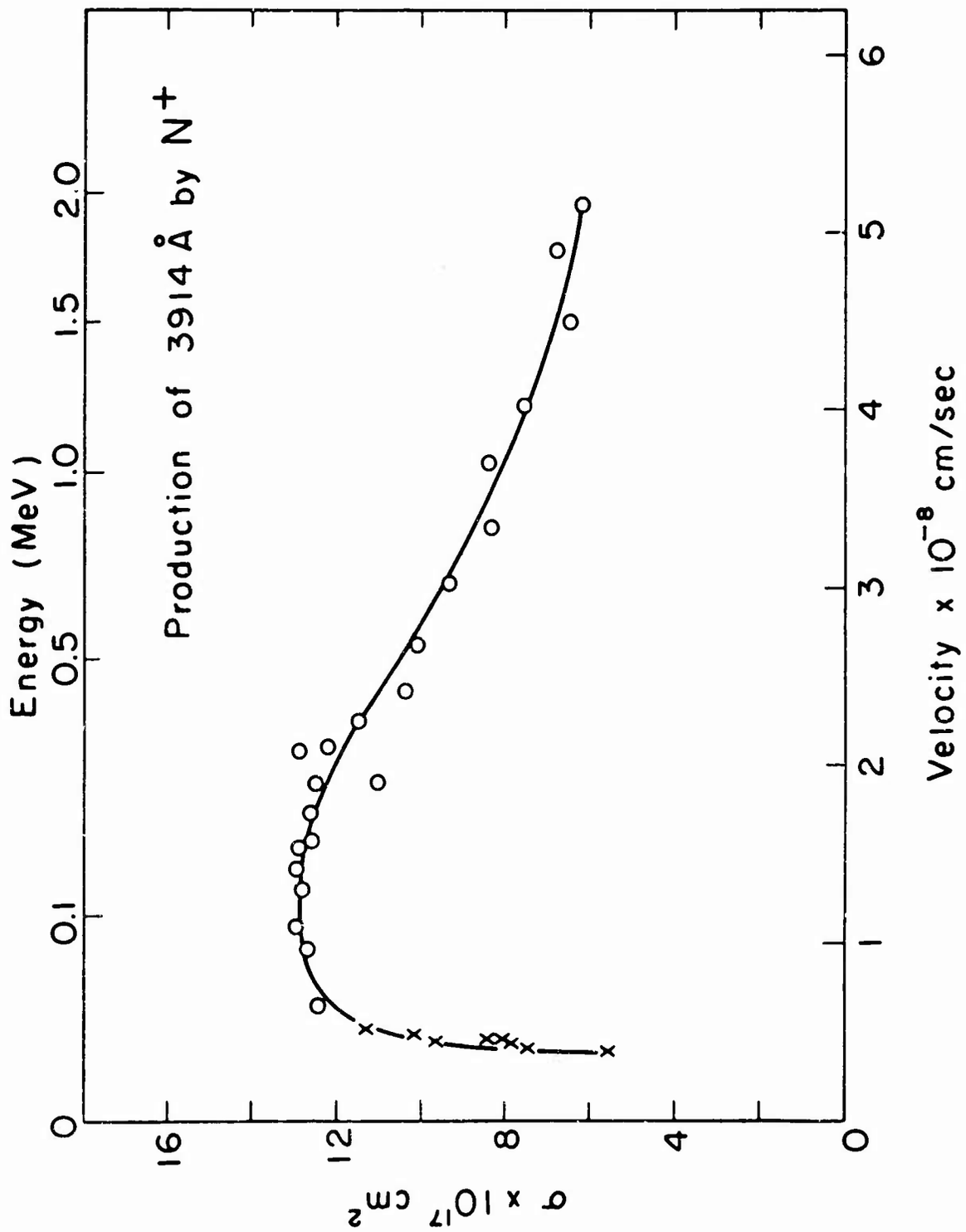

Note: The data of Sheridan and Clark (Ref. 23) plotted as (X) at low energies are observed to be consistant with the present measurements.

Figure 26. Cross Section for the Production of 3914Å Radiation in Collisions of N^+ in N_2

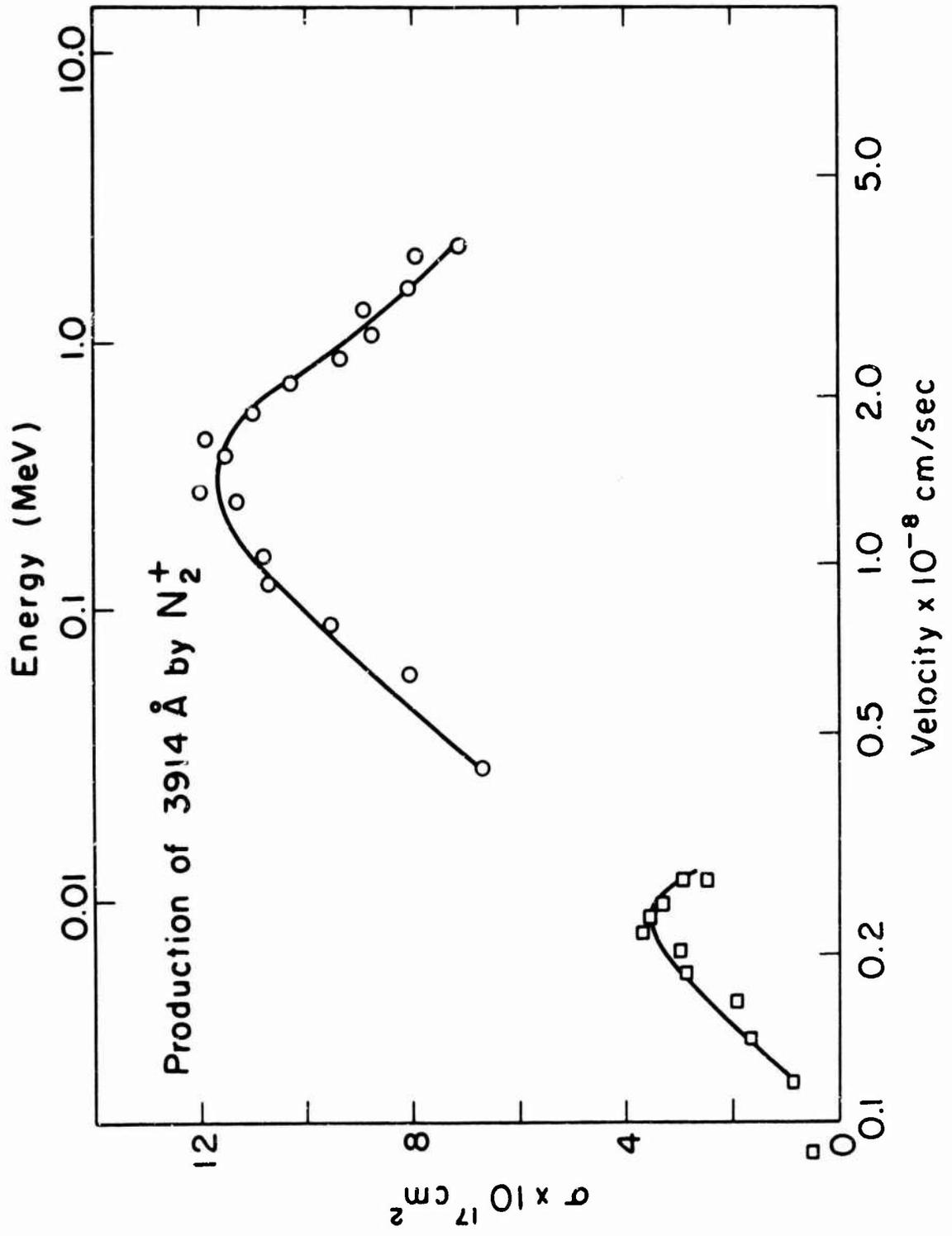

Note: The low energy points are those obtained by Doering (Ref. 25).

Figure 27. Cross Section for the Production of 3914Å Radiation in Collisions of N_2^+ in N_2 Replotted in a Logarithmic Abscissa

REFERENCES

1. W. L. Fite, J. K. Layton, and R. F. Stebbings, Experimental Studies on Heavy Ion Exchange in Air, Technical Report No. AFWL-TR-65-181, February 1966, Air Force Weapons Laboratory Kirtland Air Force Base, New Mexico.

2. J. K. Layton and W. L. Fite, Experimental Studies on Heavy Ion Exchange in Air, Technical Report No. AFWL-TR-67-2, May 1967, Air Force Weapons Laboratory, Kirtland Air Force Base, New Mexico.

3. J. K. Layton, et al., "Collision of Aluminum and Iron Atoms with Gases in the Energy Range 5 KeV - 2.5 MeV", Phys. Rev. 161, 73 (1967).

4. I. S. Dmitriev, V. S. Nikolaev, L. N. Fateeva, and Ya. A. Teplova, "Experimental Study of Electron Loss by Multiply Charged Ions in Gases", Sov. Phys. JETP 15, 11 (1962).

5. I. S. Dmitriev, V. S. Nikolaev, L. N. Fateeva, and Ya. A. Teplova, "Investigation of the Loss of Several Electrons by Fast Multiply Charged Ions", Sov. Phys. JETP 16, 259 (1963).

6. V. S. Nikolaev, I. S. Dmitriev, L. N. Fateeva, and Ya. A. Teplova, "Experimental Investigation of Electron Capture by Multiply Charged Ions", Sov. Phys. JETP 13, 695 (1961).

7. K. T. Dolder, M. F. A. Harrison, and P. C. Thonemann, "A Measurement of the Ionization Cross-Section of Ne^{+} to Ne^{2+} by Electron Impact", Proc. Roy. Soc. A 274, 546 (1963).

8. D. F. Dance, M. F. Harrison, and A. C. H. Smith, "A Measurement of the Cross Section for Production of He^{+} (2S) Ions by Electron Impact Excitation of Ground State Helium Ions", Proc. Roy. Soc. A 290, 74 (1966).

9. F. M. Bacon and J. W. Hooper, "Relative Experimental Cross Sections for Excitation of Ba^{+} Ions by Electron Impact", Vth International Conference on the Physics of Electronic and Atomic Collisions, Leningrad, 1967 (Nauka, Leningrad, 1967) p. 41.

10. W. L. Fite, "Design Considerations in Electron-Ion Experiments". To be incorporated in the final report under Air Force Weapons Laboratory Contract No. F 29601-68-C-0047.

11. J. A. R. Samson and R. B. Cairns, "A Carbon Film Scintillator Combination Suitable for the Selective Detection of Radiation in the Extreme Ultraviolet", Appl. Opt. 4, 915 (1965).

12. D. L. Ederer and D. H. Tomboulian, "The Performance of a Geiger-Mueller Counter in the 100-300Å Region", Appl. Opt. 3, 1073 (1964).

13. D. T. Stewart, "Electron Excitation Functiosn of First Negative Bands of N_2^+", Proc. Phys. Soc. Lond. A 64, 437 (1956).

14. W. F. Sheridan, O. Oldenberg, and N. P. Carleton, "Excitation of Nitrogen by Controlled Proton and Electron Impact", II International Conference on the Physics of Electronic and Atomic Collisions, Boulder, Colorado, 1961 (Abstract Book p. 159).

15. S. Hayakawa and H. Nishimura, "Measurements of Excitation Cross Section of N_2^+ First Negative Band by Electron Impact", J. Geomag. and Geoelect., 16, 72 (1964).

16. J. W. McConkey and I. D. Latimer, "Absolute Cross Sections for Simultaneous Ionization and Excitation of N_2 by Electron Impact", Proc. Phys. Soc. Lond. 86, 463 (1965).

17. J. W. McConkey, J. M. Woolsey, D. J. Burns, and F. R. Simpson, "Absolute Cross Sections for Electron Impact Excitation and Ionization of Atmospheric Gases", Vth International Conference on the Physics of Electronic and Atomic Collisions, Leningrad, 1967, (Abstract Book p. 565).

18. J. W. McConkey, J. M. Woolsey, D. J. Burns, "Absolute Cross Section for Electron Impact Excitation of 3914Å N_2^+", Planet. Spa. Sci. 15, 1332 (1967).

19. B. N. Srivastava and I. M. Mirza, "Absolute Cross Sections for Simultaneous Ionization and Excitation of N_2 by Electron Impact", Phys. Rev. 168, 86 (1968).

20. R. F. Holland, Cross Sections for Electron Excitation of the 3914Å (0,0) Band of the N_2^+ First Negative System, Los Alamos Scientific Report LA-3783, 1967.

21. N. P. Carleton and T. R. Lawrence, "Absolute Cross Sections for Excitation of Nitrogen by Protons of a Few keV", Phys. Rev. 109, 1159 (1958).

22. J. L. Philpot and R. H. Hughes, "Spectroscopic Study of Controlled Proton Impact on Molecular Nitrogen", Phys. Rev. 133, A107 (1964).

23. J. R. Sheridan and K. C. Clark, "Vibration and Rotation of N_2^+ Excited by 10-65-keV Ions", Phys. Rev. 140, 1033 (1965).

24. E. W. Thomas, G. D. Bent, and J. L. Edwards, "Cross Sections for the Formation of Excited States in a Nitrogen Target by the Impact of 0.15 to 1.0 MeV Protons", Phys. Rev. 165, 32 (1968).

25. J. P. Doering, "Cross Sections for Some N_2^+ and N_{II} Emissions Excited by 1 to 10 keV N_2^+ on N_2", Phys. Rev. 133, 1537 (1964).

UNCLASSIFIED
Security Classification

DOCUMENT CONTROL DATA - R & D

(Security classification of title, body of abstract and indexing annotation must be entered when the overall report is classified)

1. ORIGINATING ACTIVITY *(Corporate author)*
University of Pittsburgh
Department of Physics
Pittsburgh, Pennsylvania

2a. REPORT SECURITY CLASSIFICATION
UNCLASSIFIED

2b. GROUP

3. REPORT TITLE
EXPERIMENTAL RESEARCH ON COLLISIONS OF HEAVY PARTICLES AT ENERGIES UP TO 2 MeV

4. DESCRIPTIVE NOTES *(Type of report and inclusive dates)*
30 June 1967 to 30 June 1968

5. AUTHOR(S) *(First name, middle initial, last name)*
R. T. Brackman
W. L. Fite

6. REPORT DATE	7a. TOTAL NO. OF PAGES	7b. NO. OF REFS
October 1968	84	25

8a. CONTRACT OR GRANT NO.	9a. ORIGINATOR'S REPORT NUMBER(S)
F29601-67-C-0086	AFWL-TR-68-96
b. PROJECT NO. 5710	
c. Subtask: 07.003	9b. OTHER REPORT NO(S) *(Any other numbers that may be assigned this report)*
d.	

10. DISTRIBUTION STATEMENT This document is subject to special export controls and each transmittal to foreign governments or foreign nationals may be made only with prior approval of AFWL (WLRTH), Kirtland AFB, NM. Distribution is limited because of the technology discussed in the report.

11. SUPPLEMENTARY NOTES	12. SPONSORING MILITARY ACTIVITY
	AFWL (WLRTH) Kirtland AFB, NMex. 87117

13. ABSTRACT (Distribution Limitation Statement No. 2)

Three types of experiments were performed to study collision properties of ions in the energy range from approximately 50 keV to 2 MeV. The first study made measurements of the electron capture and loss cross sections of N^+, O^+, Xe^+, and U^+ in collision with N_2, O_2, Ar, and Ne. Results for stripping of electrons from the neutral atoms of the above ions were deduced from the data as well. The second study measured the cross sections for exciting the (0,0) transition of the first negative bands of N_2^+ at 3914Å on impact of Ba^+, Ba^{++}, Xe^+, O^+, N^+, and N_2^+ on N_2. In the third study an initial attempt was made to measure the cross section of electron-impact excitation of He^+ to the n = 2 state, wherein a fast beam of He^+ was passed through a space charge limited electron cloud and the 304Å photons were to be measured. While this novel approach has not yielded the desired cross section, the general approach of placing relative energy in the ion instead of in the electron when studying the interactions between ions and electrons appears to have considerable promise.

DD FORM 1 NOV 65 1473 REPLACES DD FORM 1473, 1 JAN 64, WHICH IS OBSOLETE FOR ARMY USE.

UNCLASSIFIED
Security Classification

14. KEY WORDS	LINK A		LINK B		LINK C	
	ROLE	WT	ROLE	WT	ROLE	WT
Charge exchange Heavy ions Electron capture and loss Stripping Excitation of N_2^+ at 3914Å						